Strong Motion at Port Island during the Kobe Earthquake

S.P.G. Madabhushi

CUED/D-SOILS/TR285 (1995)

STRONG MOTION AT PORT ISLAND DURING THE KOBE EARTHQUAKE

by

S.P.Gopal Madabhushi
Research Fellow (Wolfson College),
Cambridge University Engineering Dept.,
Cambridge

Abstract

It is important to understand the propagation of the stress waves through the soil strata overlying the bed rock. Several strong motion traces were recorded during the Kobe earthquake at different observation sites monitored by CEORKA (the Committee of Earthquake Qbservation and Research in the Kansai Area). At the Port Island site recordings were made in the N-S, E-W and U-D directions at four different depths. The data from this site provides an excellent opportunity to investigate the modulation of stress waves as they travel from the bed rock to the soil surface. This report concerns itself with the analysis of the data recorded at this site.

It was observed that there is significant attenuation of the peak ground acceleration in the upper strata of soil at this site. The N-S component and the E-W component during this earthquake are 180" out of phase as the strong motion reaches the soil surface. Lissajous figures of these two components were constructed at all the four depths. These figures suggest that the strong motion polarises in the N-W and S-E direction as the it approaches the soil surface. The arrival time of the U-D component induced by the P waves was compared with the arrival time of the horizontal components induced by the shear waves. As would be expected the P waves arrived earlier than the shear waves at the soil surface. Frequency analyses were carried out for strong motion recorded in both N-S and E-W directions. These analyses revealed that there is a strong attenuation of high frequency components while selective discrete frequencies are amplified as the stress waves propagate from the bed rock to the soil surface. One of the implications of this observation is that a single frequency earthquake actuators which can impart powerful strong motion to the centrifuge model may be very useful when modelling the dynamic soil-structure interaction problems with earthquake loading in a geotechnical centrifuge.

1 Introduction

The earthquake of 17 January, 1995 near Kobe city in Japan has provided strong motion records at several locations. The earthquake measured 7.2 on the Richter scale and inflicted significant damage to the prosperous city of Kobe. There were extensive liquefaction induced failures in the reclaimed areas and sea-front sites. Most notable of these failures were the quay walls which failed following liquefaction and led to failure of heavy machinery like over head cranes, gantries and even effected near by buildings. This report concerns itself with the analyses of ground motions recorded at the Port Island site which is one of the reclaimed areas.

It is known that the stress waves propagating from the epicentre undergo changes according to the medium in which they are propagating. The soil layers overlying the bed rock will modify the stress waves as they propagate towards the surface, and largely determine the type of ground motion felt at the soil surface. This is extremely important when determining the damage to the structures in different regions for the purpose of constructing the seismic zonation maps or when evaluating the performance of a particular aseismic design (for example, base isolation of structures). The effect of the modulation of the stress waves by the soil layers must be delineated from the dynamic behaviour of structure as an identical structure in different locations may perform differently based on the ground motion it receives. Only then can we determine either the performance of buildings and map damaged structures in an earthquake effected region or determine the efficacy of an aseismic design based on the prevalent earthquake codes in that region. This immediately prompts us to study the modulation of stress waves as they travel from bed rock to the soil surface.

Strong motion records at different observation sites in Kobe were recorded by CEORKA (the Committee of Earthquake Qbservation and Research in the Kansai Area). The overall distribution of the CEORKA observation sites can be seen in Fig.l. In this figure the position of the Port Island site can also be seen. The specifications of the seismometers used in recording the ground motions are presented in Table 1. Also the soil conditions at all of the CEORKA sites are presented in Table 2 with the

Data plots of CEORKA sites

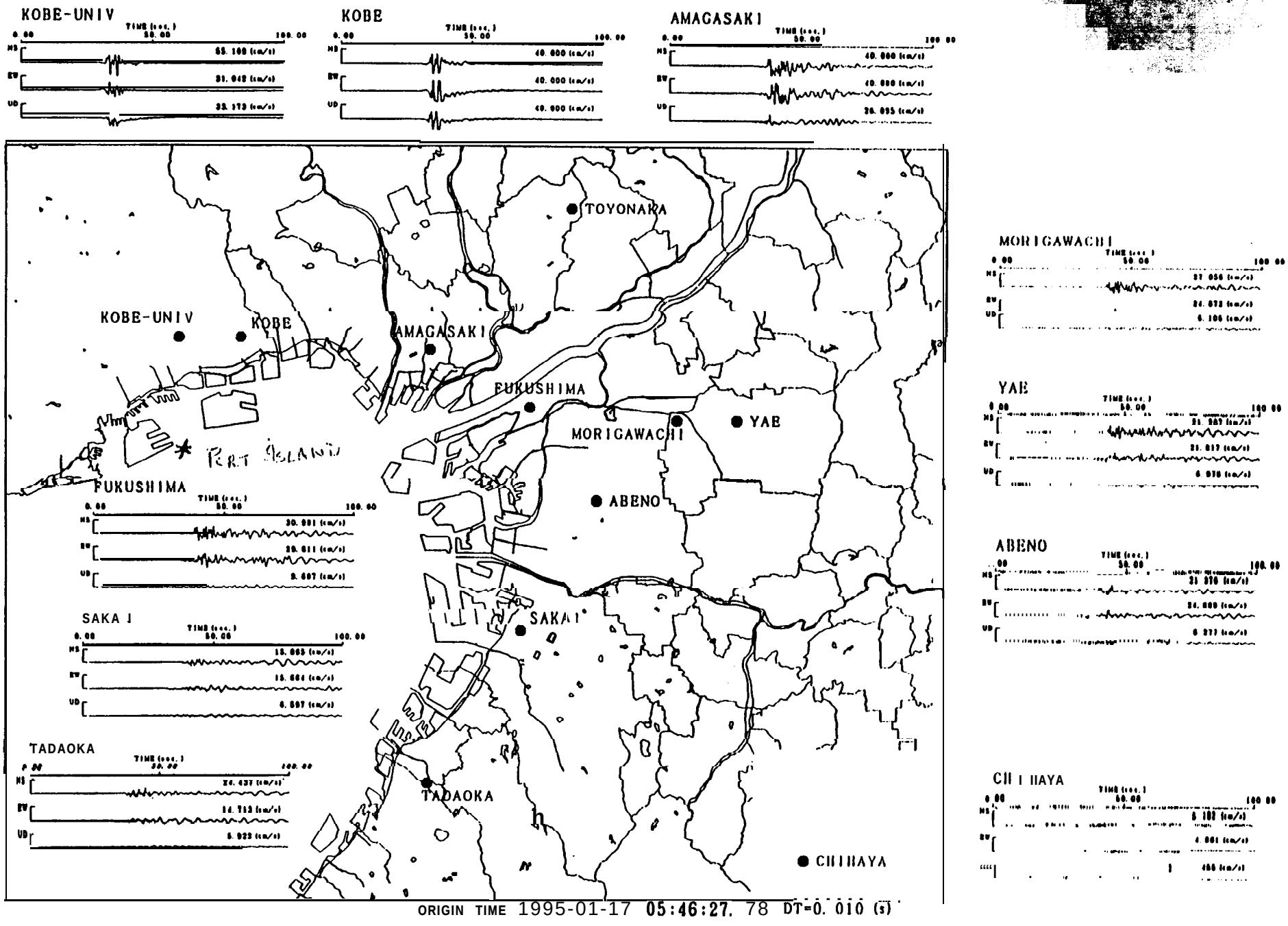

Fig. 1 Location of the CEORKA observation sites in the Kobe City

Table 1 Recording System of CEORKA

		Standard	Wide Range
Seiemometer	Frequency Range	4Osec. ~ 70Hz	
	Full Scale (10 Volt.)	Low Gain 40cm/s High Gain 1cm/s Acc. 1,000cm/s2	Low Gain 100cm/s High Gain 5cm/s
Recorder	Channel	3	6
	Sampling	50,100, or 200Hz	
	Pre-Trigger	5~30sec.	
	Triger Type	Dynamic Level, Logical	
	Interface	RS-232C(Up to 38,400bps.)	
	Clock	Radio Wave Correctted	

Wide range type systems are installed at the Kobe-Univ., the Chihaya, and the Yae sites.

Table 2 Infonnations of Sites

Site	Latitude	Longitude	Altitude	Soil Conditions
Kobe-Univ.	N34.725	E135.240	110m	Mesozoic granit
Kobe	N34.725	E135.281	25m	Late Pleistocene fan deposits
Amagasaki	N34.718	E135.408	0m	Thick Holocene deposits
Fukushima	N34.687	E135.474	0m	Thick Holocene deposits
Morigawachi	N34.680	E135.572	1m	Thick Holocene deposits
Yae	X34.680	E135.612	3m	Thick Holocene deposits
Tovonaka	X34.801	E135.501	55m	Pliocene deposit
Sakai	N34.564	E135.462	2m	Thin Holocene! deposits
Tadaoka	X34.480	E135.408	12m	Thin Holocene deposits
Chihaya	X34.439	E135.659	280m	Mesozoic granit
Abeno	N34.636	Ei35.5 19	12m	Late Pleistocene deposits
(Port Island)	X34.670	E135.208	4m	Reclaimed land

latitude, longitude and the altitude of each recording station. Note in this table that the soil type at the Port Island site is reclaimed land All of the data were uncorrected and no processing was performed on the data.

2 Port Island Site Specifications

Port Island site was chosen for the present analysis as strong motion was recorded at different depths at this site. This will enable us to study the modulation of the strong motion as it propagates from the bed rock to the soil surface. As mentioned earlier this site is in the reclaimed area where liquefaction of soil is a major concern. The plan view of the Port Island area is shown in Fig.2. In this figure the actual site at which the instruments were located is marked by a solid dot (•). Accelerations were recorded at four different depths namely 83m, 32m, 16m below ground level and at the soil surface. The soil profile at this site is presented in Fig.3. The soil properties and the stress wave velocities in each of the strata shown in Fig.3 are presented in Table 3. At each of the depths the acceleration-time histories were recorded in the N-S (North-South) direction, E-W (East-West) direction and U-D (Up-Down) direction.

3 Strong motion records

The acceleration-time histories recorded at the Port Island site in the N-S direction, E-W direction and U-D direction are presented in Figs.4 to 6. In each of these figures the acceleration-time histories at different depths are presented. These figures show the modulation of the strong motion as it travels towards the soil surface. In Fig.4 the strong motion in the N-S direction show a reduction of high frequencies as they travel towards the soil surface. In Sec.6 of this report we shall consider this aspect in some detail. Also the amplitude of the acceleration decreases significantly in the soil strata lying between the ground surface and 16m depth. Looking at Fig.5 we can draw a similar conclusion that the high frequency components of the ground motion in the E-W direction are attenuating as the waves travel to the soil surface and the amplitude of

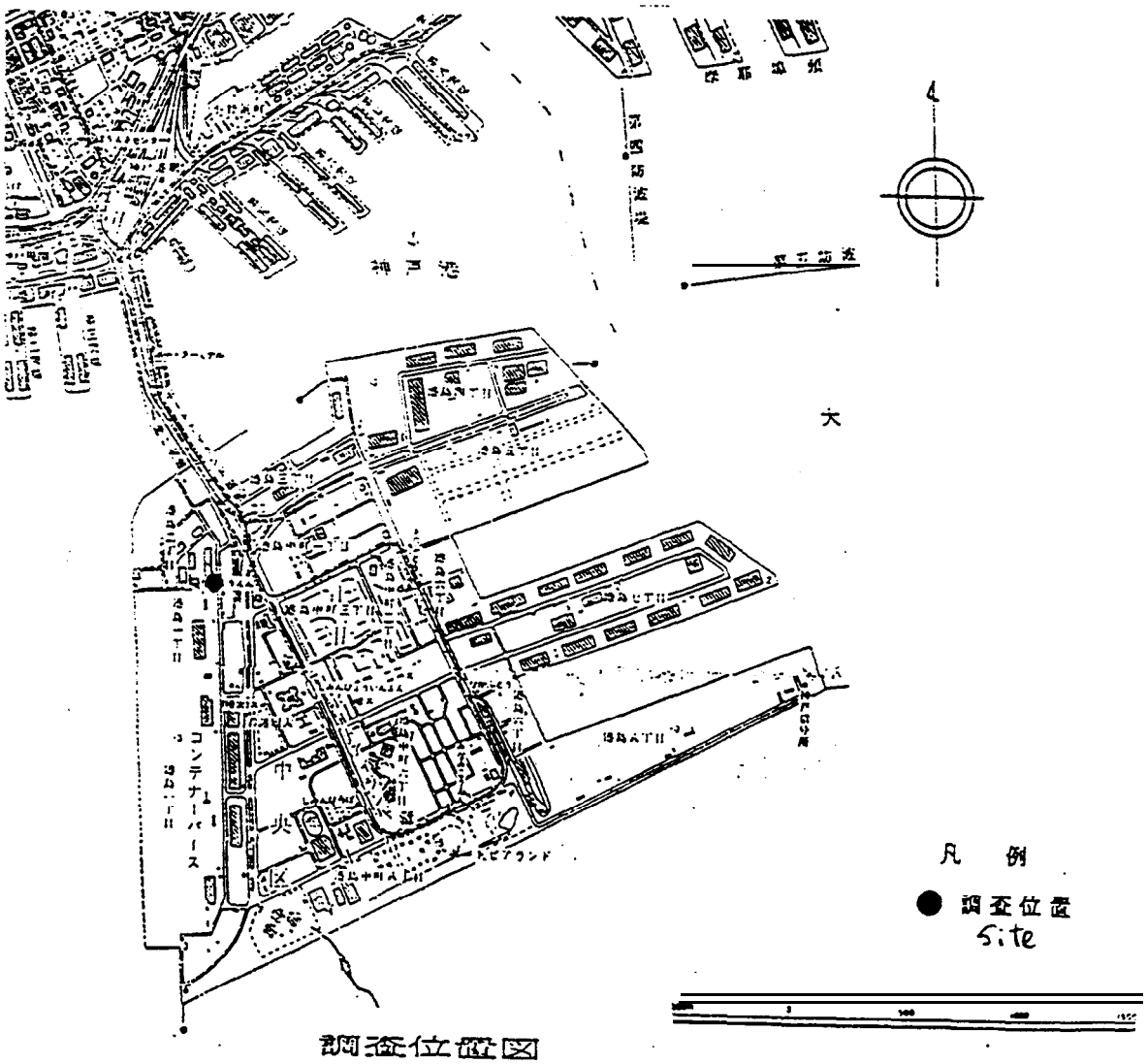

Fig.2 Plan view of the Port Island area

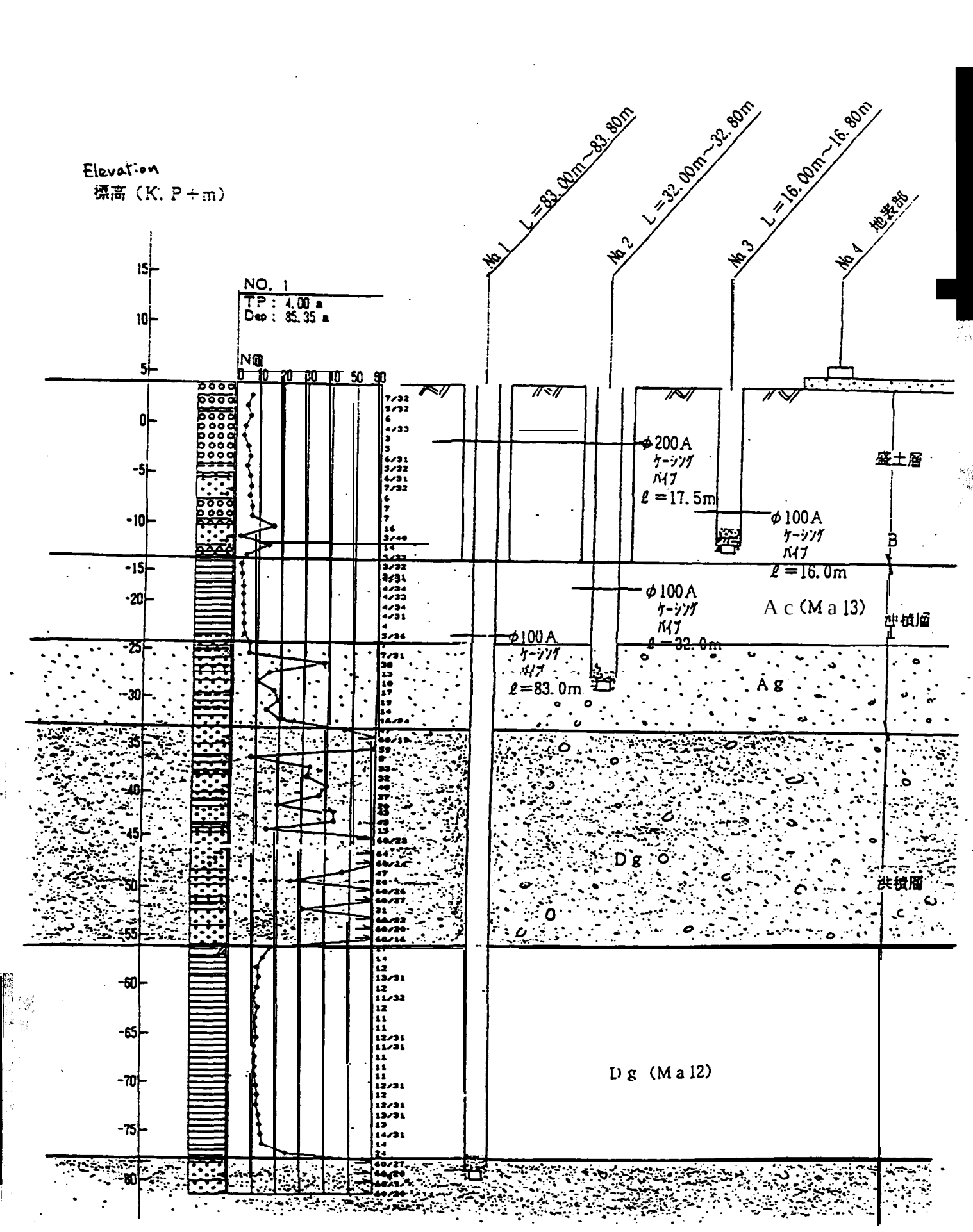

Fig. 3 Soil profile at the recording station in Port Island

Sensor

Table 3 Soil Informations of the Port Island Site

Depth 深度 (m)	主な土質		P S 検層結果 P波速度 Vp(km/s)	S波速度 Vs(km/s)	SPT 平均N値 (MIN～MAX)	Poisson Ratio ポアソン比 σ
0 ～ 2.0	砂礫 Gravel	埋立土砂 Reclaimed	0.260	0.170	5.2(3.6～6.6)	0.127
2.0～ 5.0	砂礫 Grave		0.330			0.319
5.0～ 12.6	砂礫 Gravel		0.780	0.210	6.5(2.3～16)	0.461
12.6～ 19.0	Sand with Gravel 礫混り砂		1.48			0.490
19.0～ 27.0	粘土	沖積粘土層 Ma13	18	0.18	3.5(2.8～4)	0.488
27.0～ 33.0	砂 Sand	第1洪積 砂礫層	1.33	0.245	13.5(4.2～38)	0.482
33.0～ 50.0	Sand with Gravel 礫混り砂, 砂		1.53	0.35	36.5(8 ～94.7)	0.479
50.0～ 61.0	砂 Sand		1.61	0.350	61.9(17～112.5)	0.475
61.0～ 79.0	粘土 Clay	洪積粘土層 Ma12		0.303	11.7(10.3～13)	0.482
79.0～(85.0)	礫混り砂	第2洪積砂礫層	2.0	0.32	68.0(13.5～200)	0.487

the acceleration is decreasing markedly in the top 16m of the soil strata. One of the reasons for this may be due to partial liquefaction resulting in a partial loss of soil stiffness. This will result in a lower transmissibility of the stress waves thus resulting in smaller peak accelerations near the soil surface. However, no pore pressure measurements were made at the site to confirm the partial liquefaction hypothesis. Fig.8 also shows attenuation of high frequency components in the U-D direction as the vertical accelerations travels to the soil surface. Also the vertical accelerations show a remarkable amplification as they approach the soil surface.

In Table 4 the peak accelerations in each direction are tabulated. This table summarises the observations made in the above paragraph on the attenuation of amplitude of the accelerations as the strong motion approaches the soil surface.

Table 4 Peak ground accelerations at the Port Island site

	N-S direction (gals)	E-W direction (gals)	U-D direction (gals)
GL-00m	341.2	284.3	555.9
GL-16m	564.9	543.2	789.5
GL-32m	543.6	461.7	200.0
GL-83m	678.8	302.6	186.7

on surface

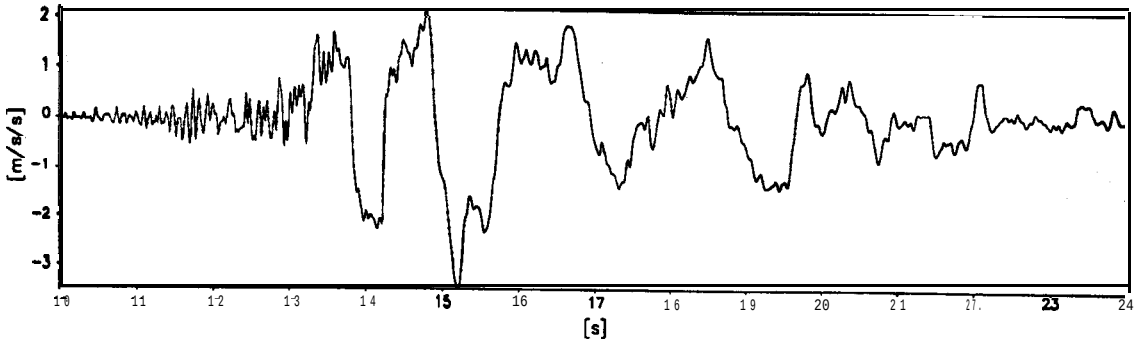

16m below ground level

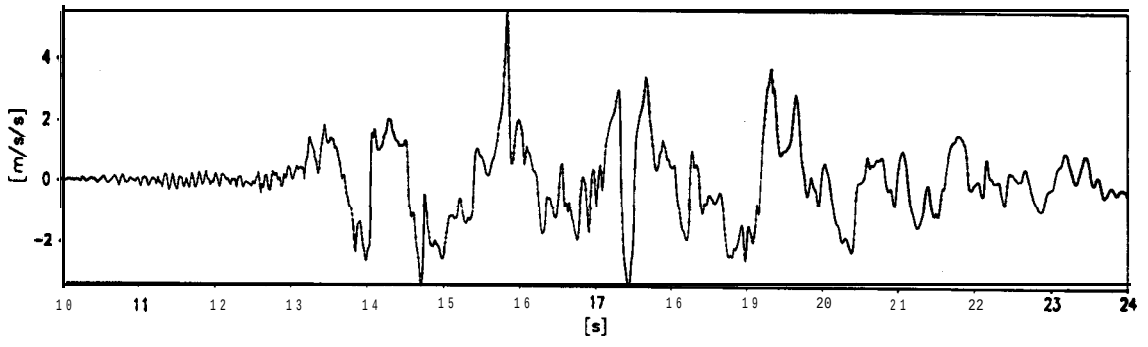

32m below ground level

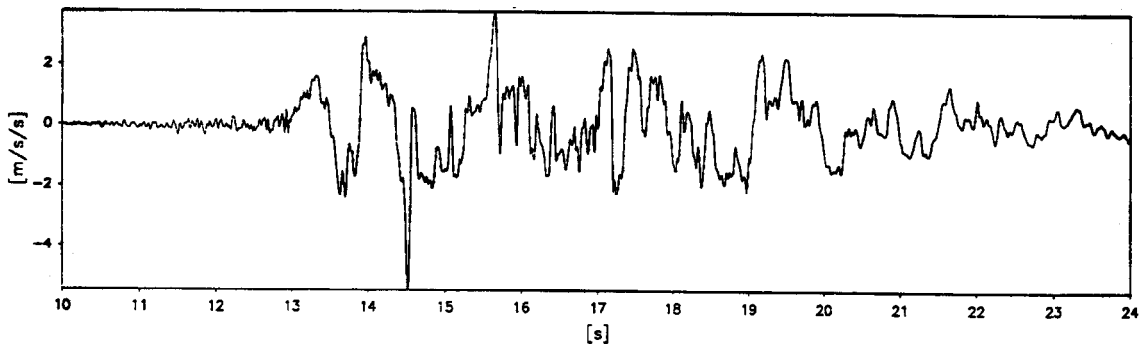

83m below ground level

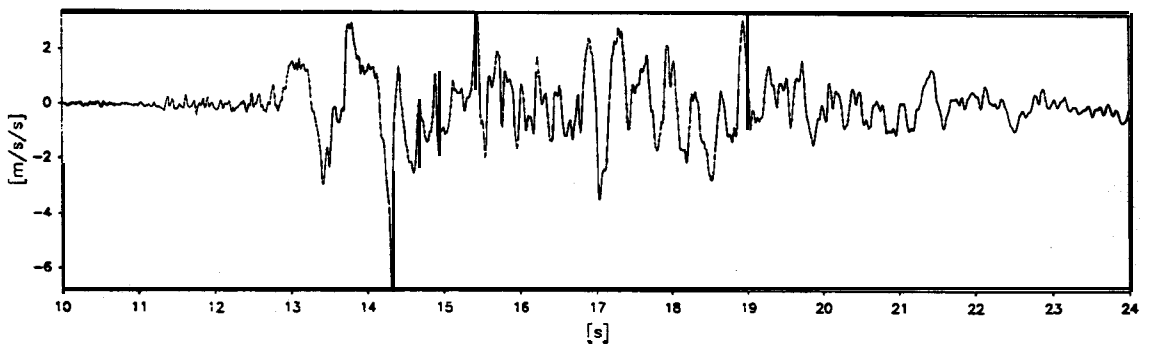

Port Island – Seismograph records at different depths

TEST MODEL FLIGHT	**Direction: N-S** **TIME RECORDS**		FIG.NO. **4**

on surface

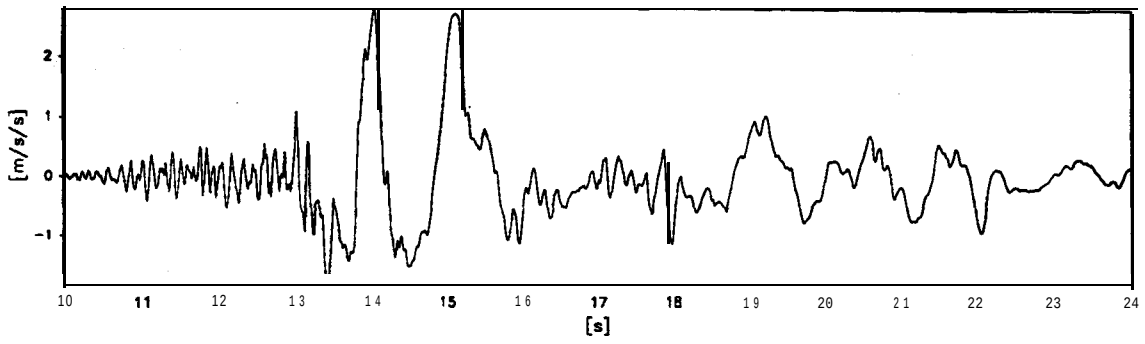

16m below ground level

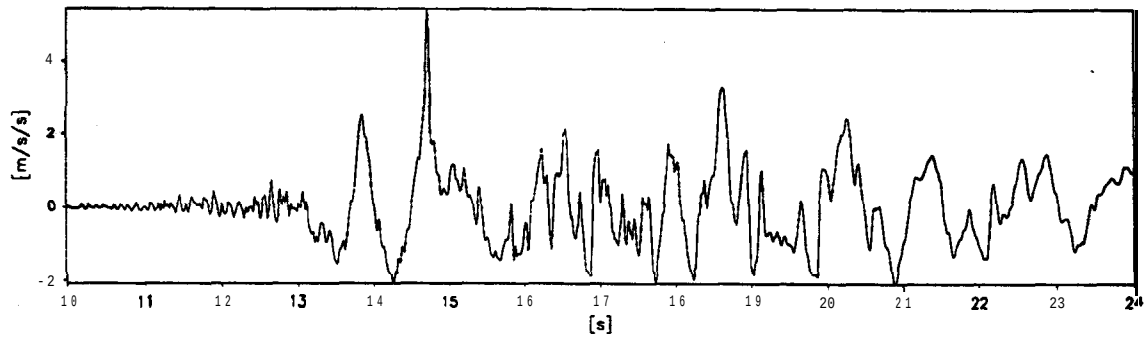

32m below ground level

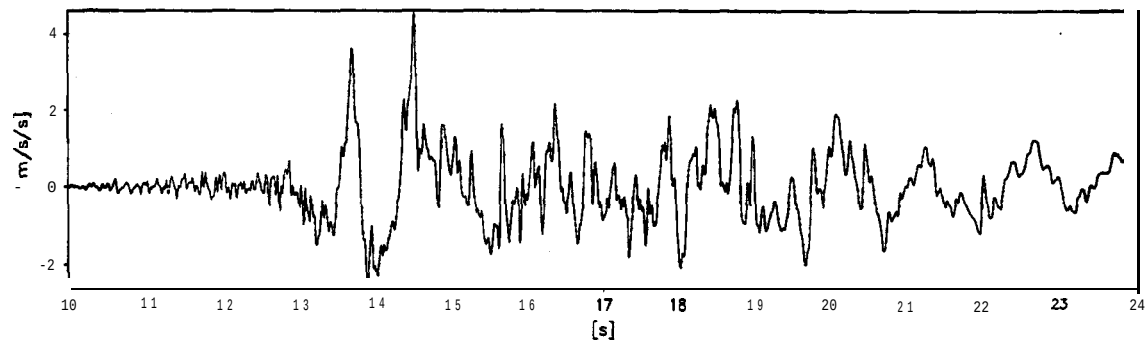

83m below ground level

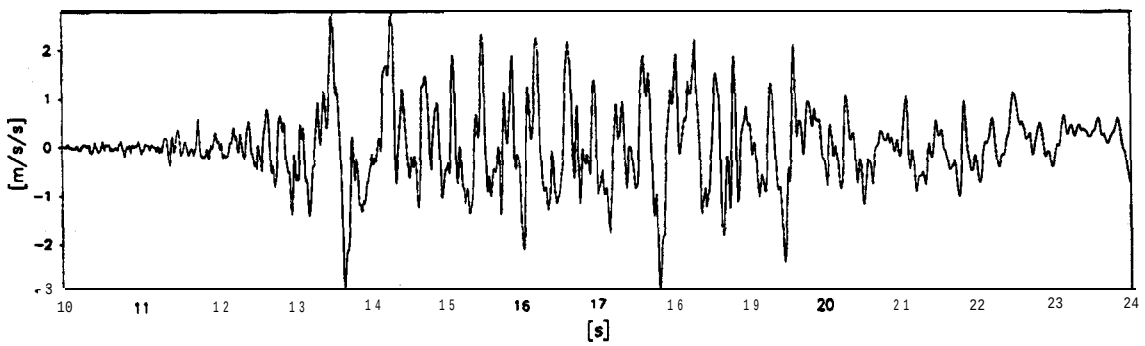

Port Island – Seismograph records at different depths

TEST MODEL FLIGHT		Direction: E-W **TIME RECORDS**		FIG.NO. **5**

on surface

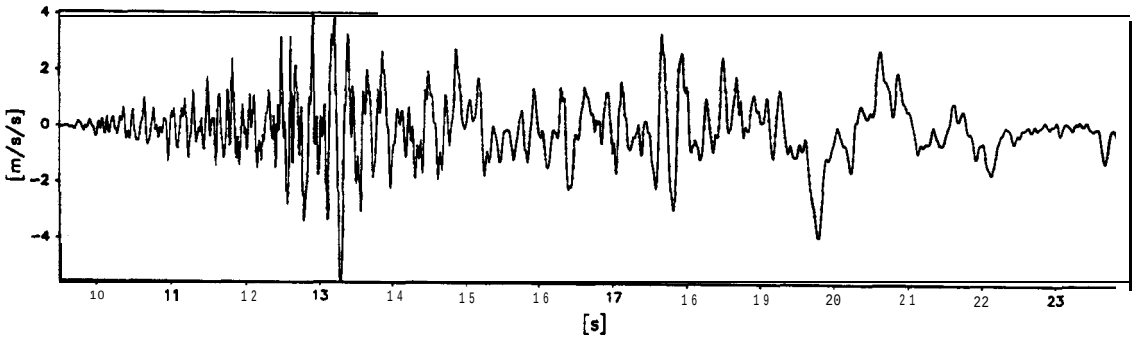

16m below ground level

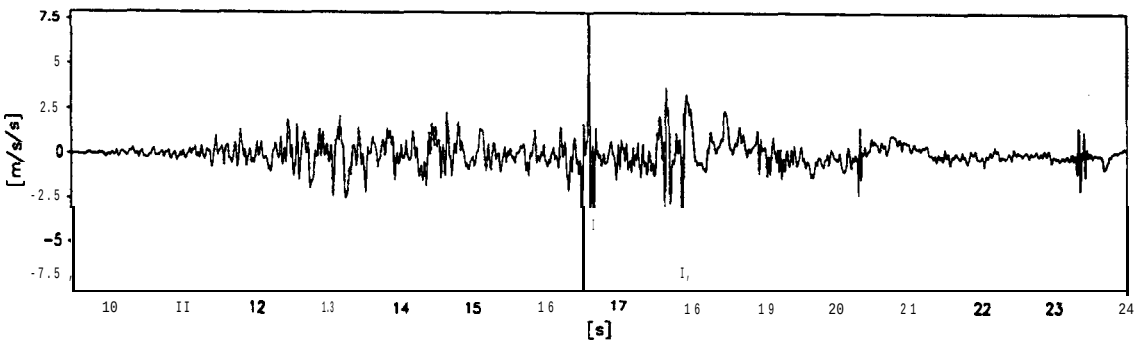

32m below ground level

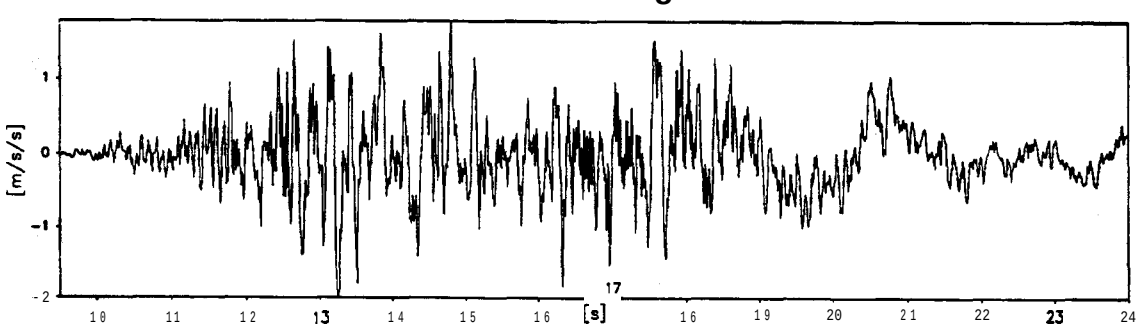

83m below ground level

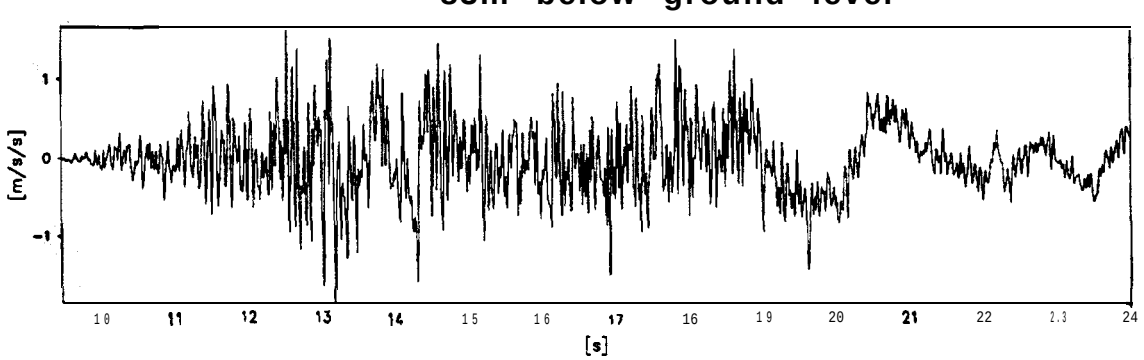

Port Island — Seismograph records at different depths

TEST MODEL FLIGHT		Direction: **U-D** **TIME RECORDS**		FIG.NO. **6**

4 Phase relationship between the N-S and E-W components

In this section we shall investigate the phase relationship between the N-S component and E-W component of the ground motion. In Fig.7 these two components recorded at the ground level are shown. From this figure it can be seen that the N-S component and E-W component are approximately 180” out of phase. This suggests that the peak acceleration in the North direction occurs at the same time as the peak acceleration occurs in the West direction. To study this further Lissajous figure was constructed by plotting the N-S component along the x-axis and the E-W component along the y-axis as shown in Fig.8. From this figure it can be seen that the resultant acceleration field acting on the soil body near the surface lies predominantly in the N-W and S-E direction.

In Fig.9 the N-S component and E-W component at the depth of 16m are shown. As in Fig.8 it is possible to see that the N-S component and E-W component are 180” out of phase. The Lissajous figure for this case is presented in Fig.10. While the overall picture is presented in this figure it was observed that the two components have a phase difference of 180° during the first half of the earthquake and the phase difference increases to 270” in the second half of the earthquake. This is reflected in the Lissajous figure as the number of points along the x-axis increases.

In Fig. 11 the N-S and E-W components recorded at a depth of 32m are shown. In this case the above components are 180” out of phase for approximately the first 2 seconds of the earthquake. The phase difference after this time is not clear. The Lissajous figure for this case is shown in Fig.12. Again the overall picture is presented in this figure. It was observed that the two components show a phase difference of 180° during the first 2 seconds or so and phase difference after this time is not clear.

Similar figures for the components at the depth of 83m are presented in Figs.13 and 14. From these figures conclusions similar to the above case may be drawn.

Comparing the Lissajous figures for all the four depths presented in Figs.8,10,12 and 14 we can observe that as the stress waves are propagating towards the soil surface the

resultant acceleration field is polar-king in the N-W and S-E direction. One of the reasons for this may be that the earthquake motion has led to the generation of excess pore pressures causing a partial liquefied soil in the upper strata. The loss of stiffness in a local region may render the site anisotropic and causing the strong motion to polarise in one direction. Also it is possible that the reclaimed land is actually subjected to tortional motion which can only be confirmed with more instruments along any one horizontal plane.

data points plotted per complete transducer record

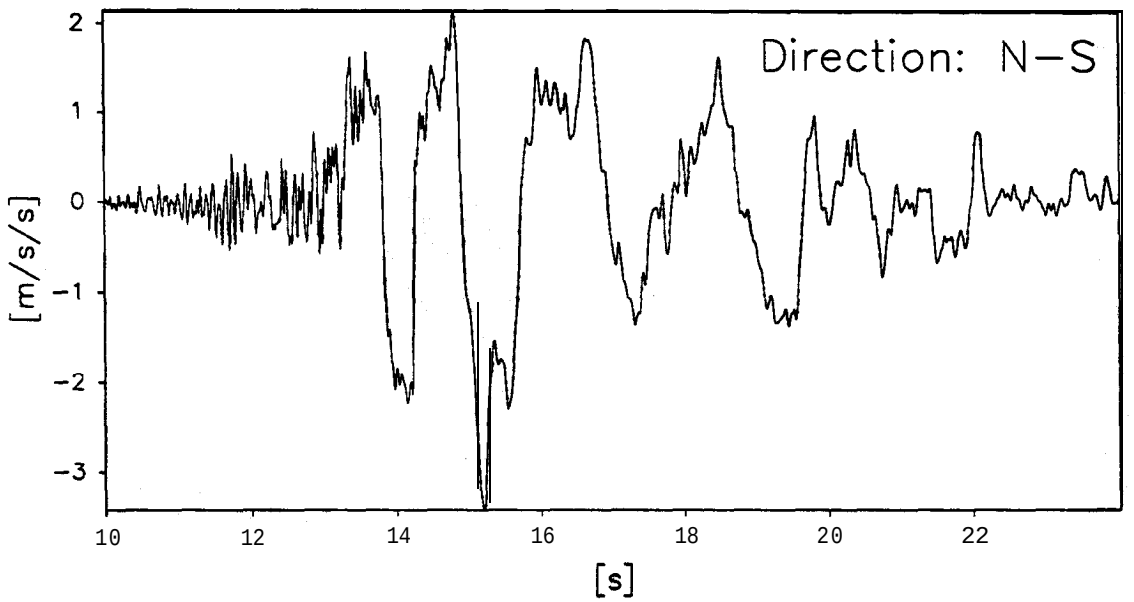

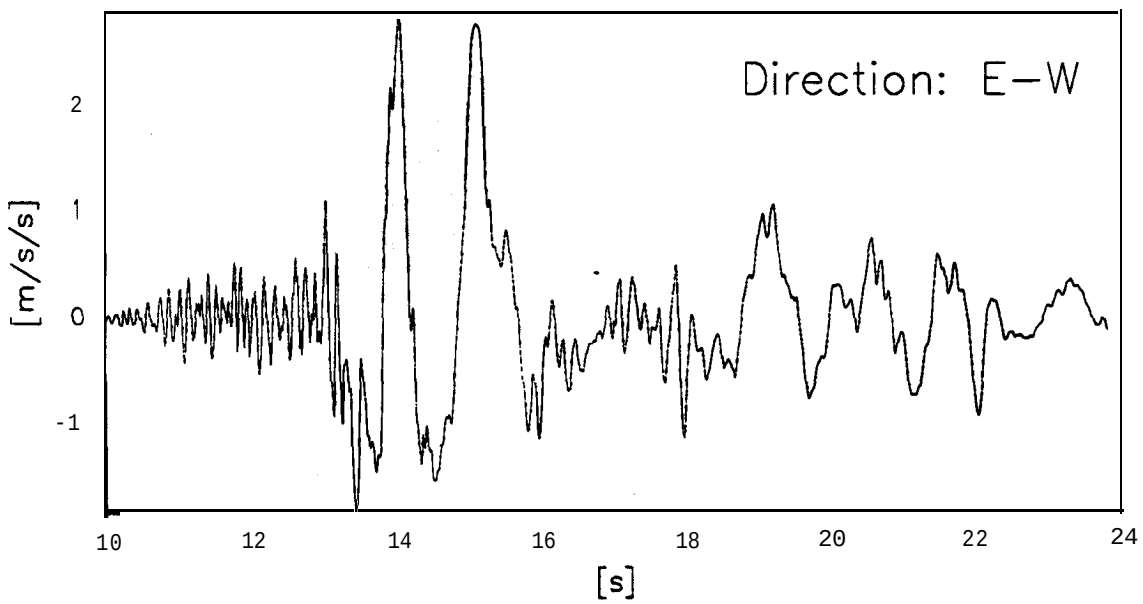

Port Island – **Seismograph near ground level**

TEST MODEL FLIGHT		**TIME RECORDS**		FIG.NO. 7

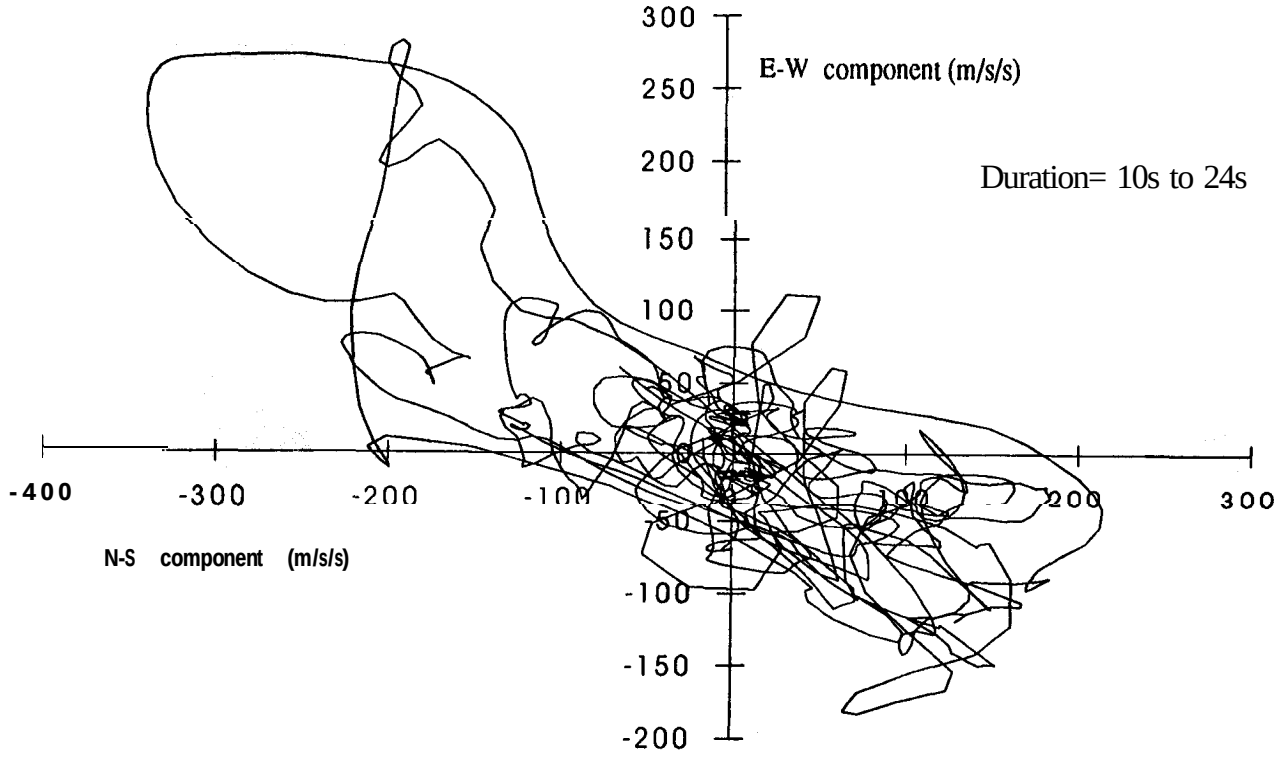

Fig.8 Lissajous plot between the N-S and E-W components
at surface level

data points plotted per complete transducer record

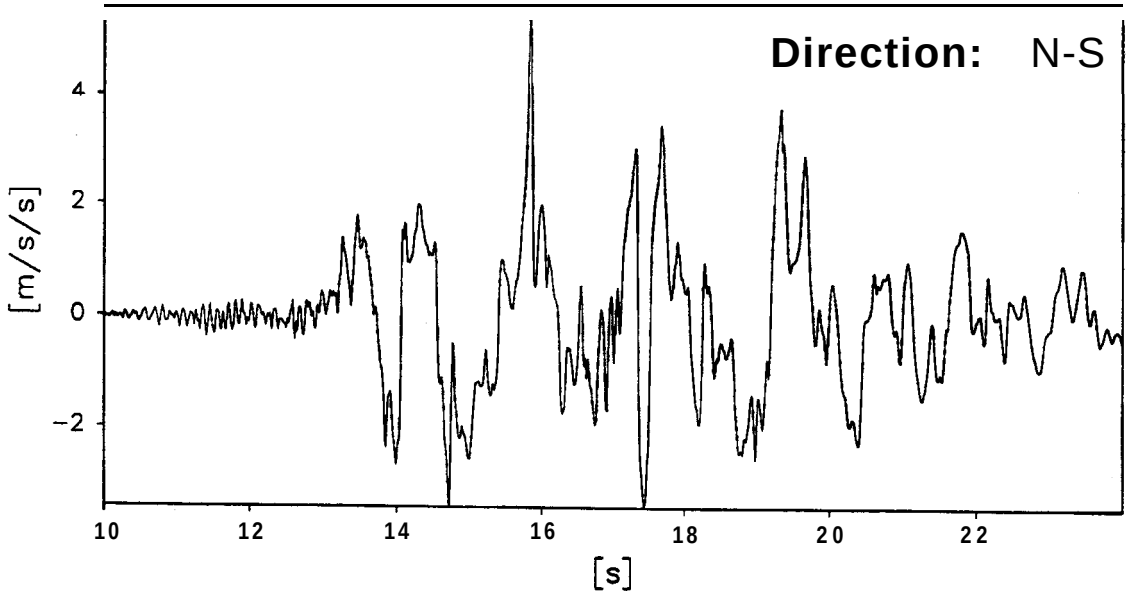

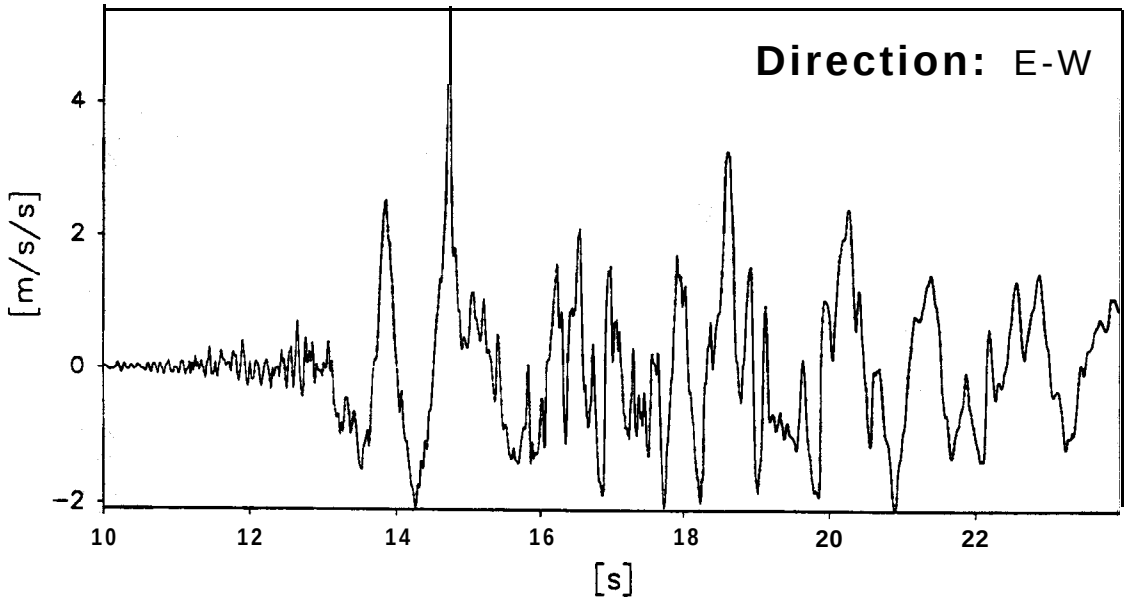

Port Island – Seismograph 16m below ground level

TEST MODEL FLIGHT		TIME RECORDS		FIG.NO. 9

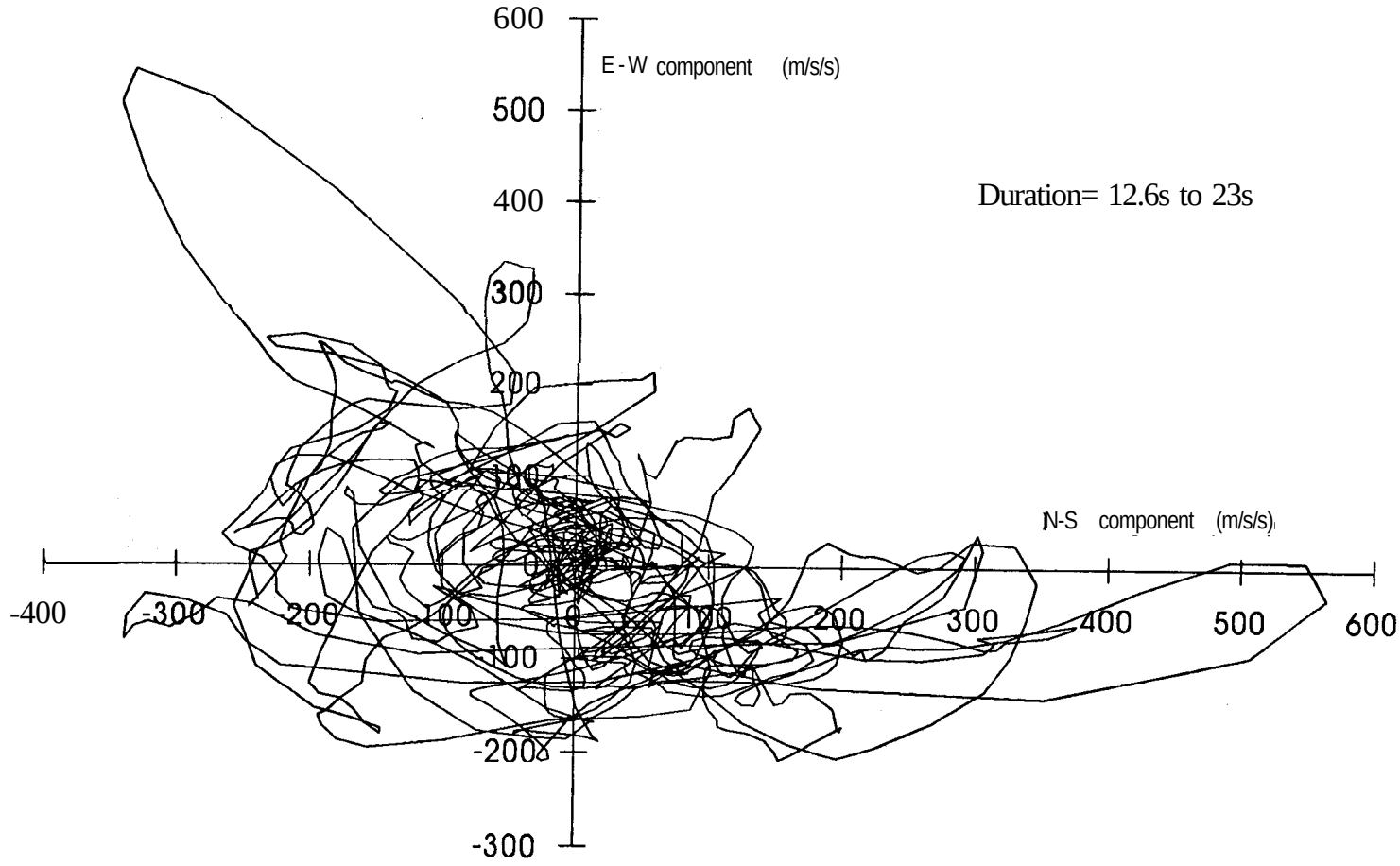

Fig. 10 Lissajous plot between the N-S and E-W components
at 16m below ground level

data points plotted per compete transducer record

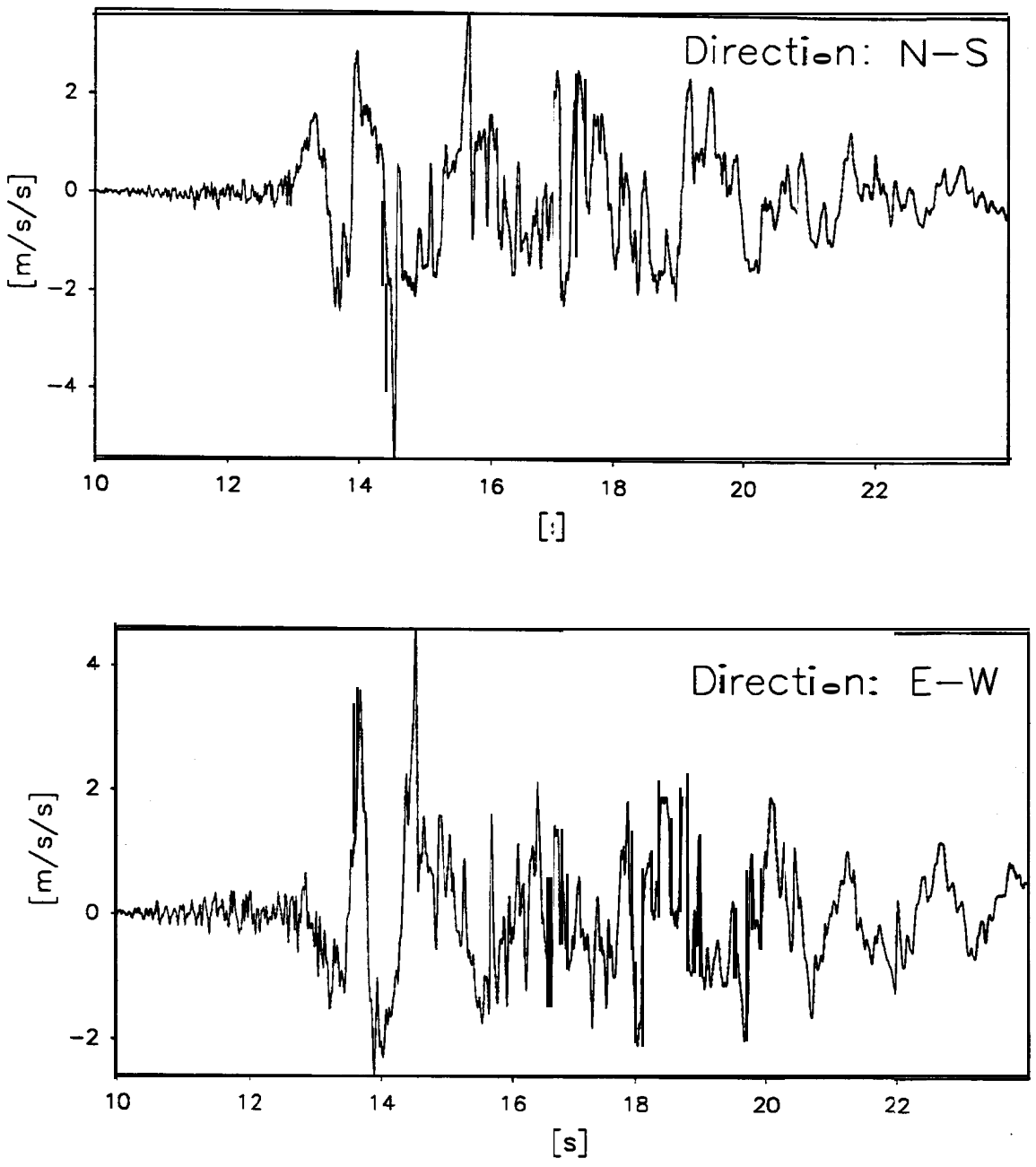

Port Island – Seismograph 32m below ground level

TEST MODEL FLIGHT		TIME RECORDS		FIG.NO. 11

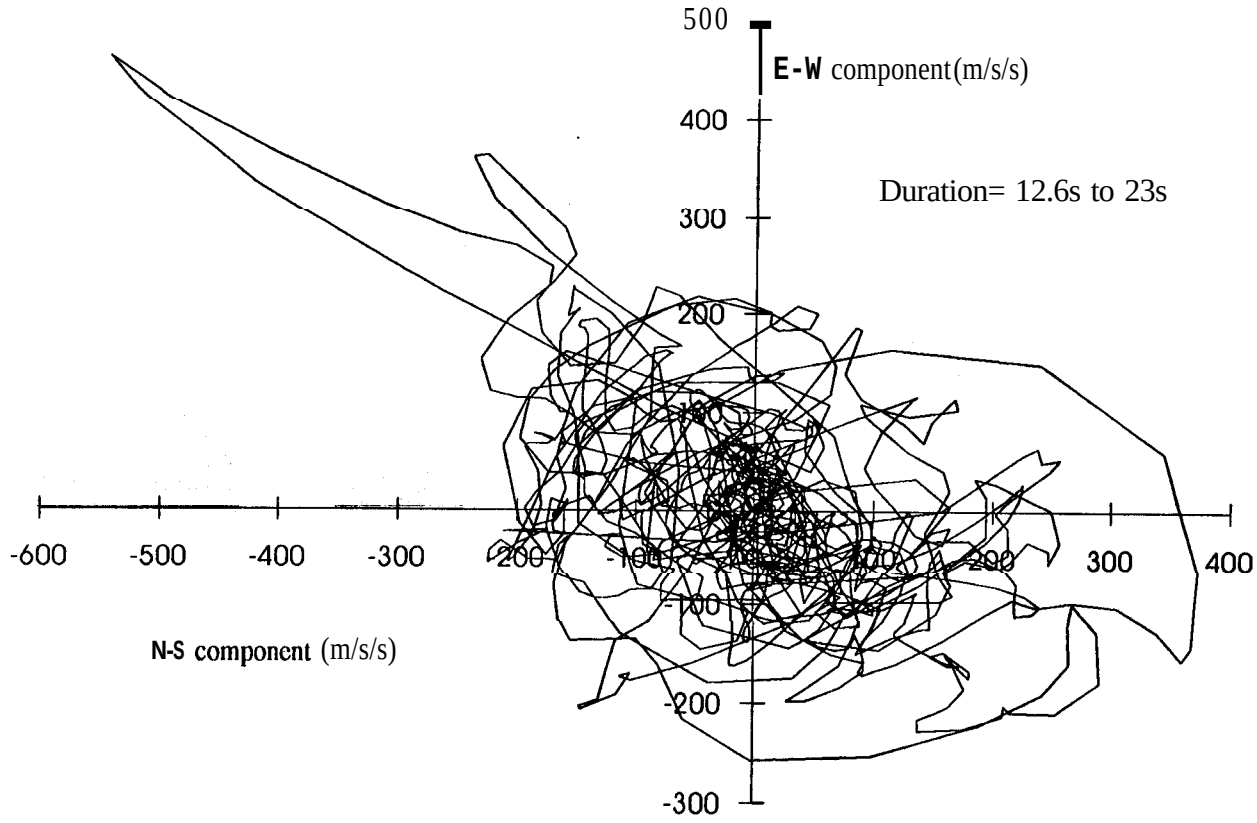

Fig. 12 Lissajous plot between the N-S and E-W components
at 32m below ground level

data points plotted per complete transducer record

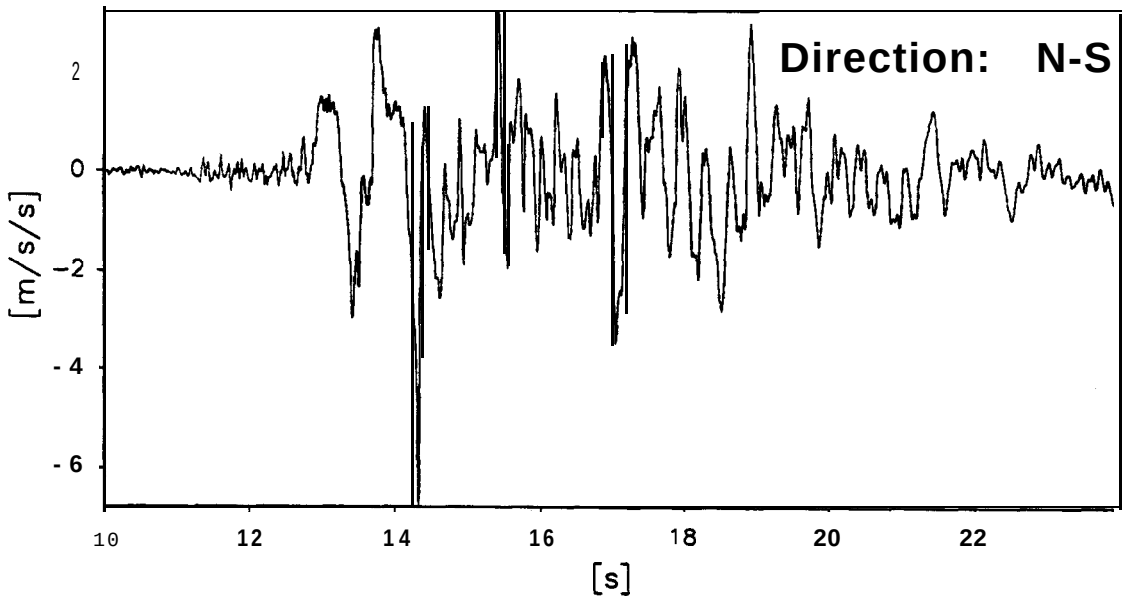

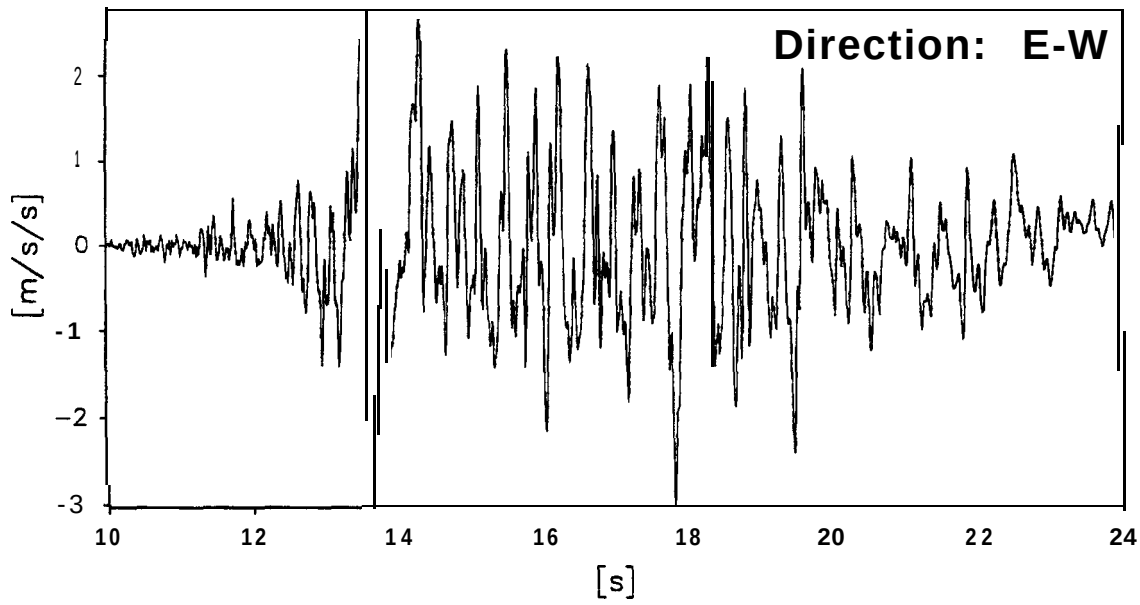

Port Island — Seismograph 83m below ground level

TEST MODEL FLIGHT		TIME RECORDS		FIG.NO. 13

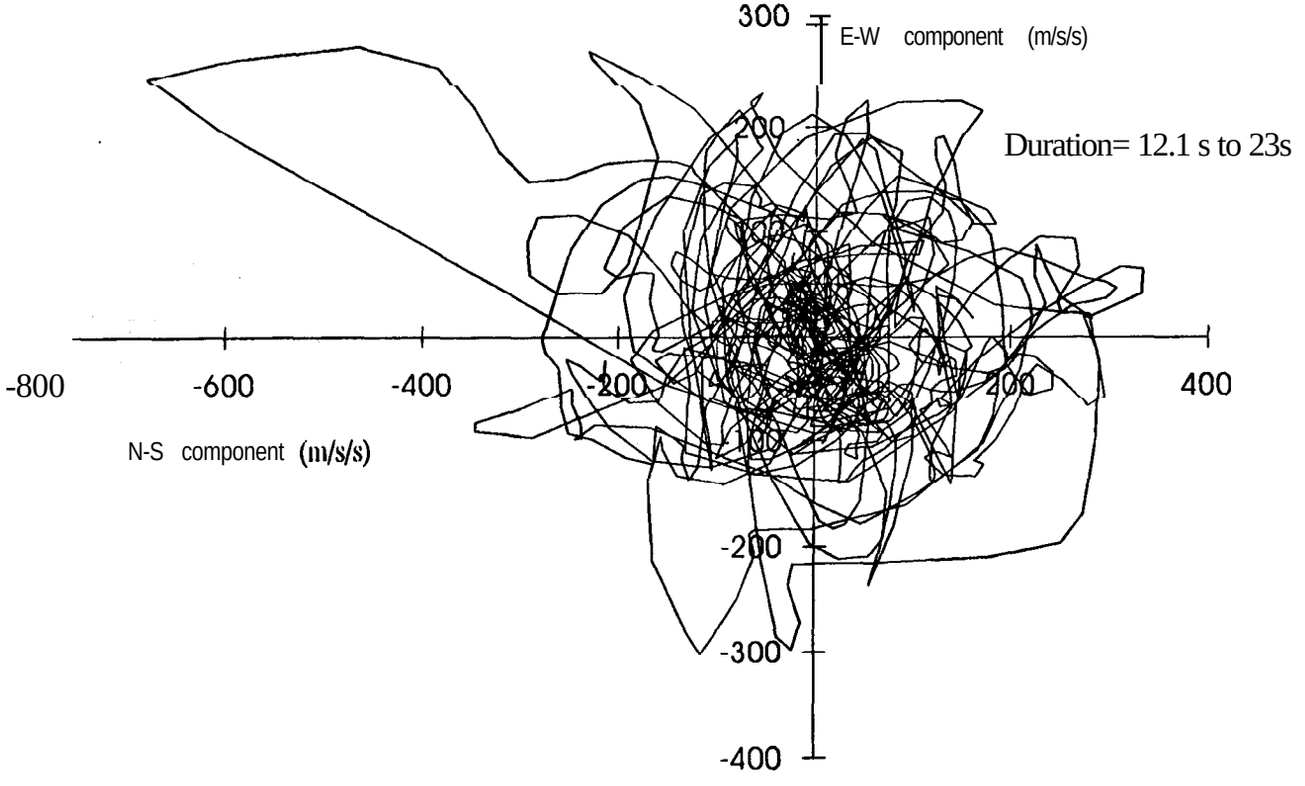

Fig.14 Lissajous plot between the N-S and E-W components
at 83m below ground level

5 Arrival of vertical accelerations relative to horizontal accelerations

The horizontal accelerations within the soil layer overlying the bed rock arise due to the vertically propagating horizontal shear waves (S_h waves). The vertical accelerations in the soil layer result from the Primary waves (P waves). In Table 3 the stress wave velocities for all the soil strata at the recording site are presented. The shear wave velocities are significantly lower than the primary wave velocities. From this it follows that the P-Waves must arrive at the surface earlier than the S_h waves.

In Fig.15 the U-D component recorded at the depth of 83m below ground level is superposed on the trace recorded in the N-S direction. A similar plot showing the superposition of the U-D component and the E-W component at this depth is presented in Fig.16. In both these figures the peak accelerations in the horizontal direction (both N-S and E-W) and vertical directions lie relatively close to each other. In Fig.17 the U-D component recorded at the ground level is superposed on the trace recorded in the N-S direction. A similar plot showing the superposition of the U-D component and the E-W component at the ground level is presented in Fig.18. In Figs. 17 and 18 the peak vertical accelerations occur significantly before the peak accelerations in the horizontal direction (both N-S and E-W). This confirms that the vertical accelerations are induced by the P-waves while the S_h waves cause the horizontal accelerations.

data points plotted per complete transducer record

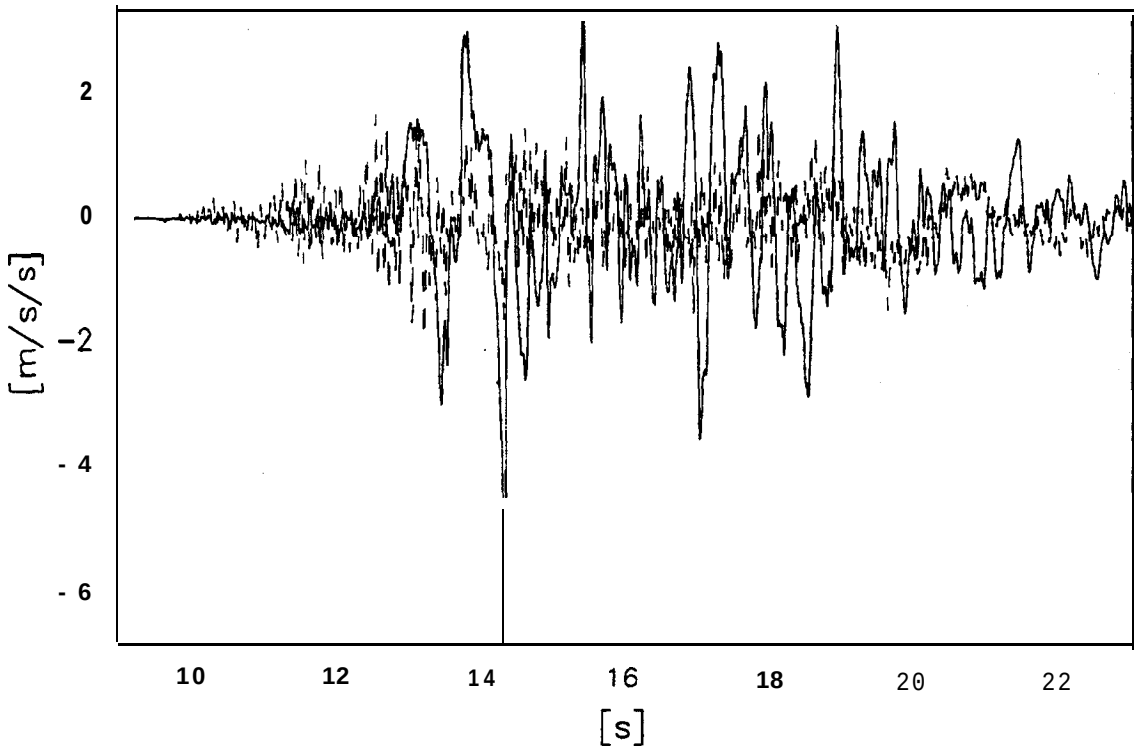

TEST MODEL FLIGHT		TIME RECORDS		FIG.NO. 15

data points plotted per complete transducer record

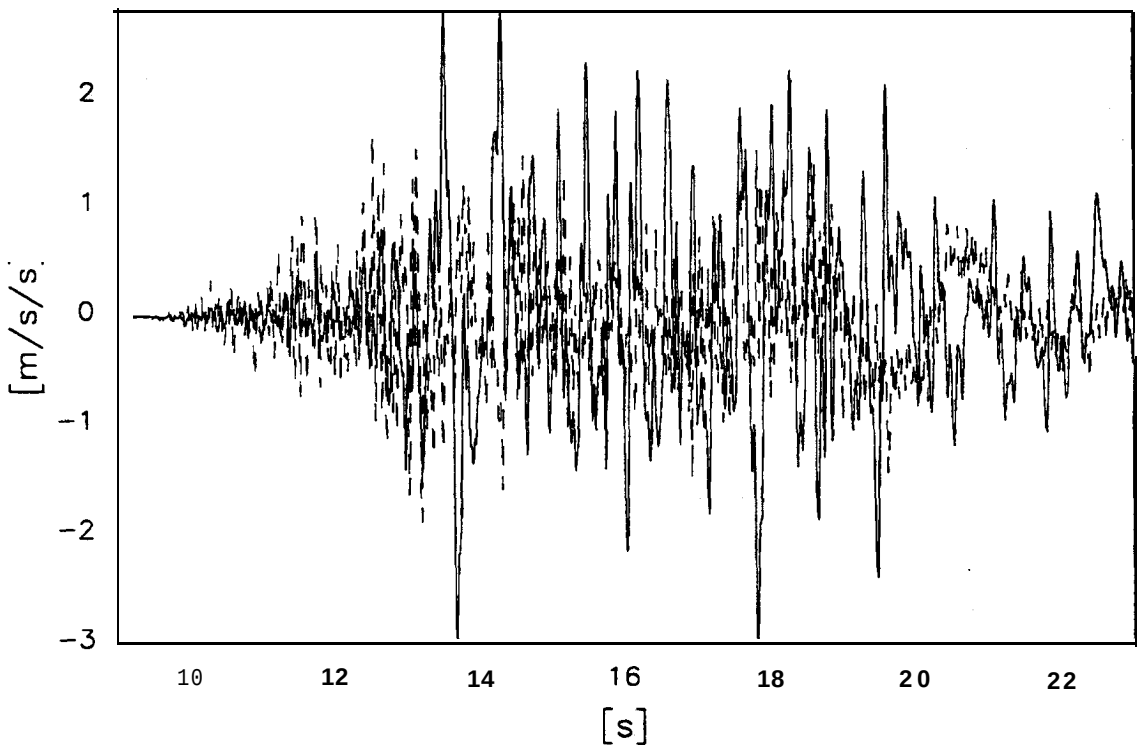

Port Island – Seismographs 83m below ground level

Direction: E-W ——

Direction: U–D ---

TEST MODEL FLIGHT		TIME RECORDS		FIG.NO. 16

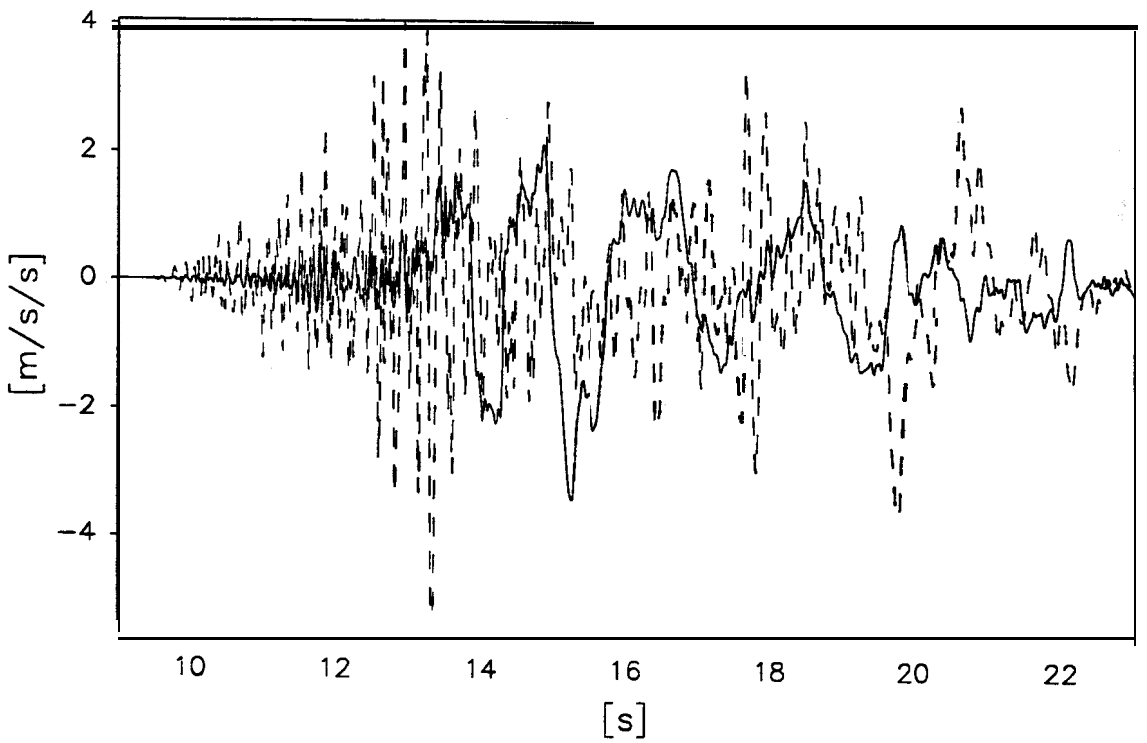

Port Island – Seismographs at ground leve

Direction: N–S ——

Direction: U–D – – –

TEST MODEL FLIGHT		TIME RECORDS		FIG.NO. 17

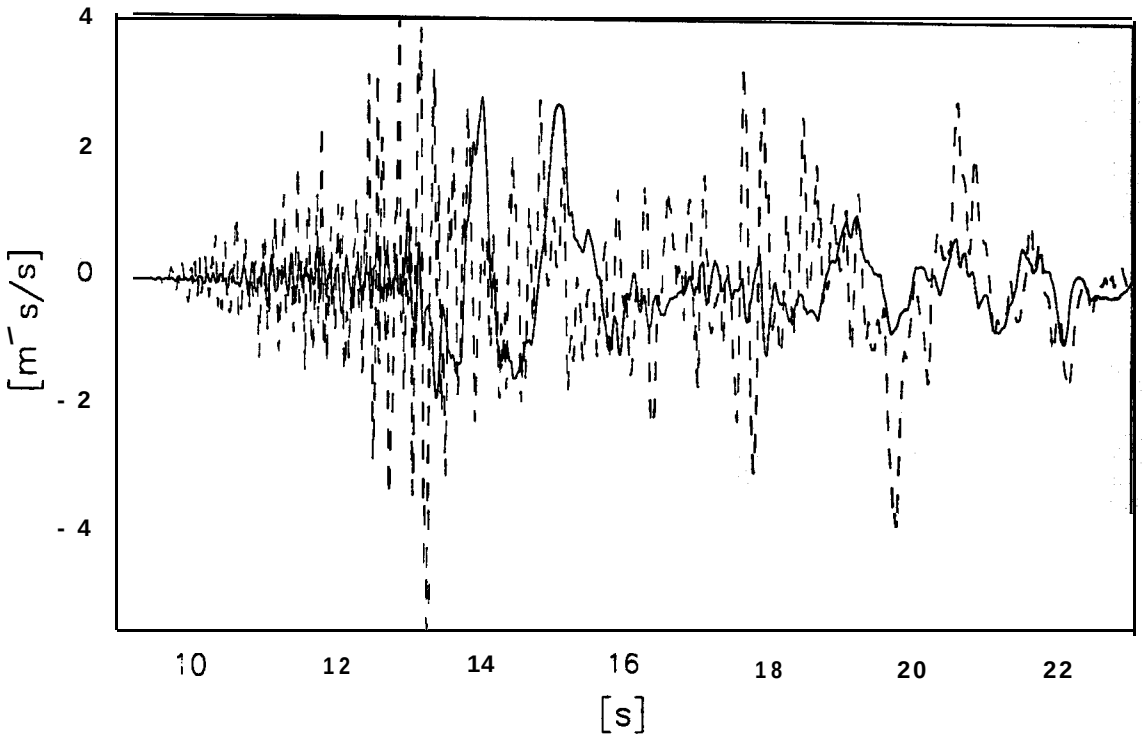

Port Island – Seismographs at ground level

Direction: E-W ——

Direction: U-D ---

TEST MODEL **FLIGHT**		**TIME RECORDS**	FIG.NO. **18**

6 Frequency Analysis of ground motion in the N-S direction

It was observed in Sec.3 that the strong motion suffers an attenuation of the high frequency components as it propagates from the bed rock towards the soil surface. In this section this feature is considered in some detail. Frequency analyses were carried out by using the Discrete Fast Fourier Transform (DFT) method. In Figs.19 to 22 the frequency analysis of the N-S component and the actual time trace of the strong motion at different depths are presented.

The frequency analysis of the strong motion recorded at the depth of 83 m shows significant components at various frequencies between 0 to 10 Hz as seen in Fig.19. Some of these high frequencies are filtered by the time the strong motion arrives at the depth of 32m. This is seen in Fig.20 which reflects the attenuation of the 2.8 Hz component and amplification of the 0.5 and 0.75 Hz components. As the strong motion travels upwards to the depth of 16 m the 0.5 and 0.75 Hz components show further amplification as seen in Fig.21. As the strong motion reaches the soil surface there is some attenuation of the 0.5 and 0.75 Hz components as seen in Fig.22. The 2.8 Hz component and all of the high frequency components suffer extensive attenuation in this region as reflected in Fig.22. Comparing the frequency analyses in Figs. 19 and 22 the dramatic filtering of the high frequency components is visualised.

The effect of partial liquefaction was proposed as a possible reason for the attenuation of amplitude of the ground motion in the upper strata at this site. It is clear by comparing Figs.19 and 22 that this attenuation is not effecting all the frequency components in the same way. The 2.8 Hz components suffers extensive attenuation in the top 16m of soil strata bringing its magnitude from $0.15 m/s^2$ at 16 m depth to 0.02 m/s^2 at the soil surface (a reduction of 86.6%). The 0.5 Hz component suffers an attenuation from 0.22 m/s^2 to 0.18 m/s^2 in the same soil strata (a reduction of 22.2%).

data points plotted per complete transducer record

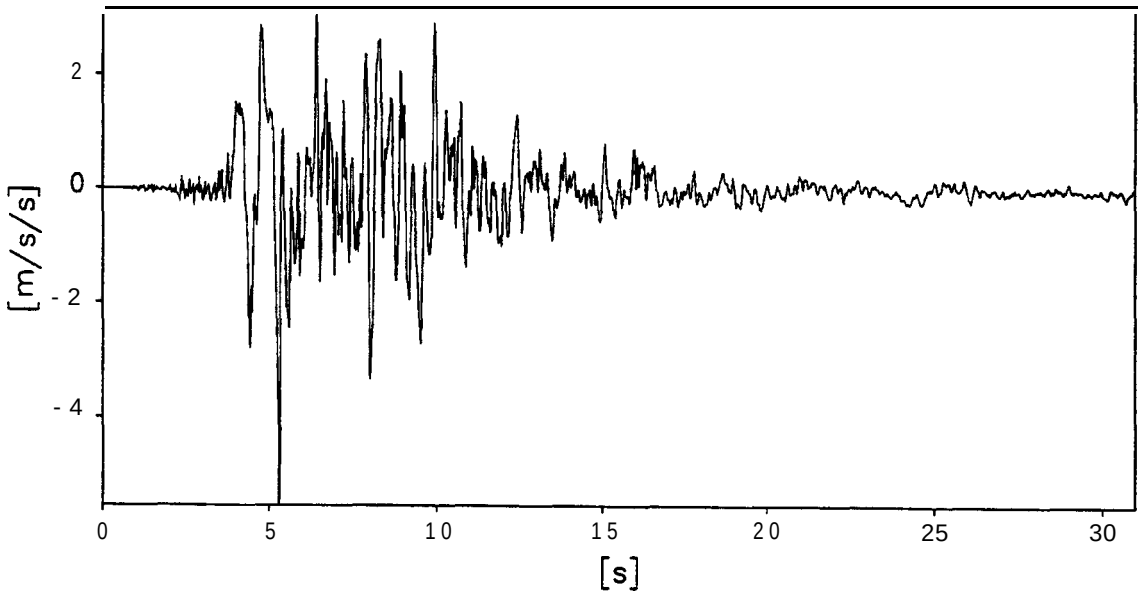

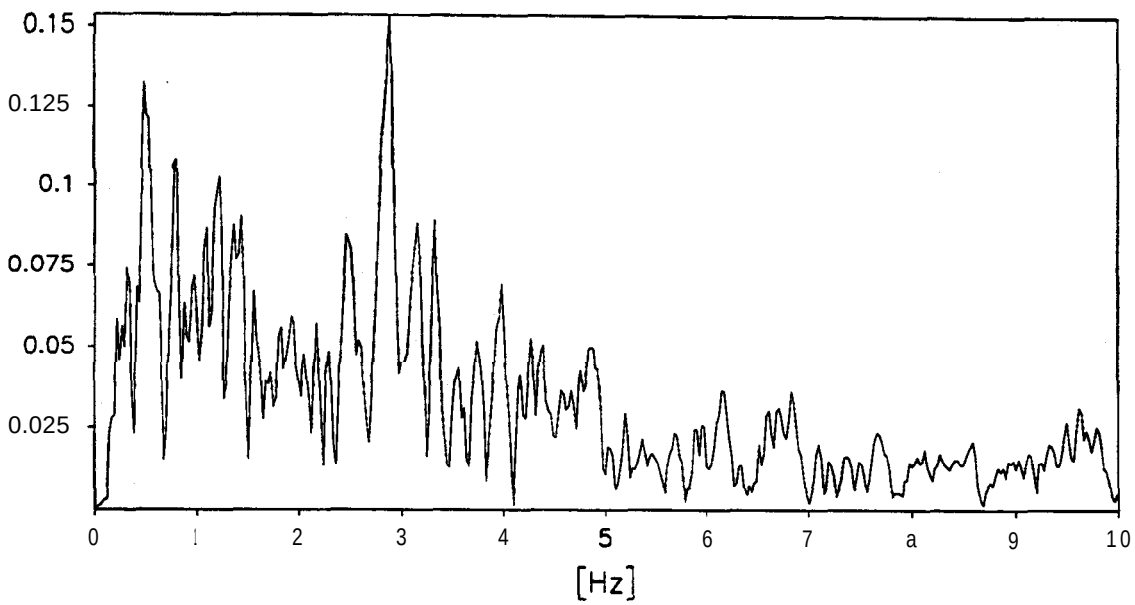

Port Island — Seismograph 83m below ground level

Direction: N-S

TEST MODEL FLIGHT		TIME RECORDS		FIG.NO. 19

data points plotted per complete transducer record

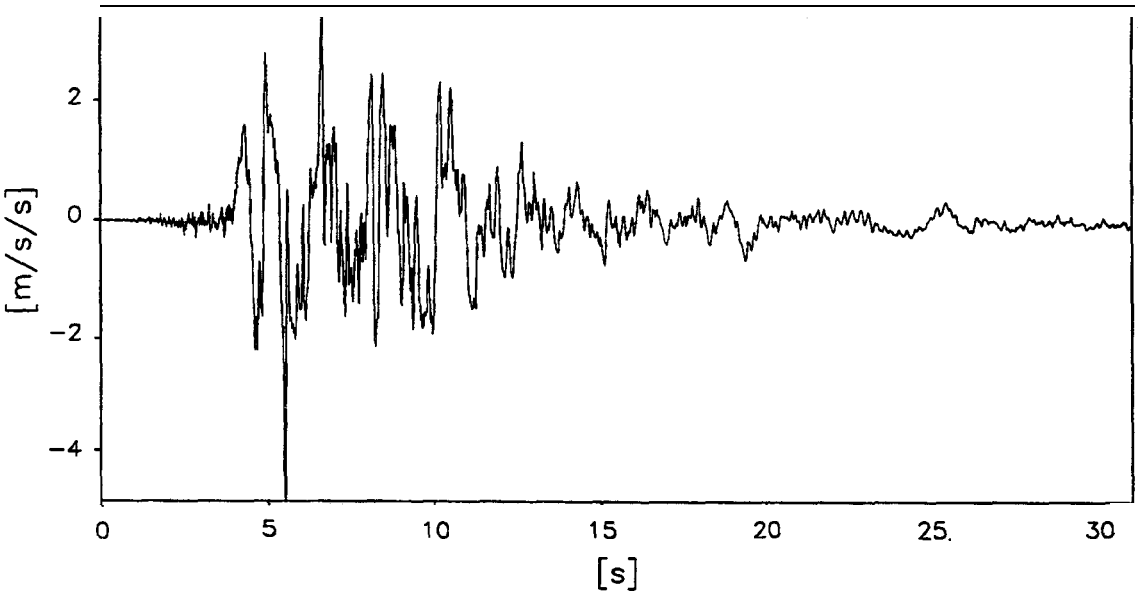

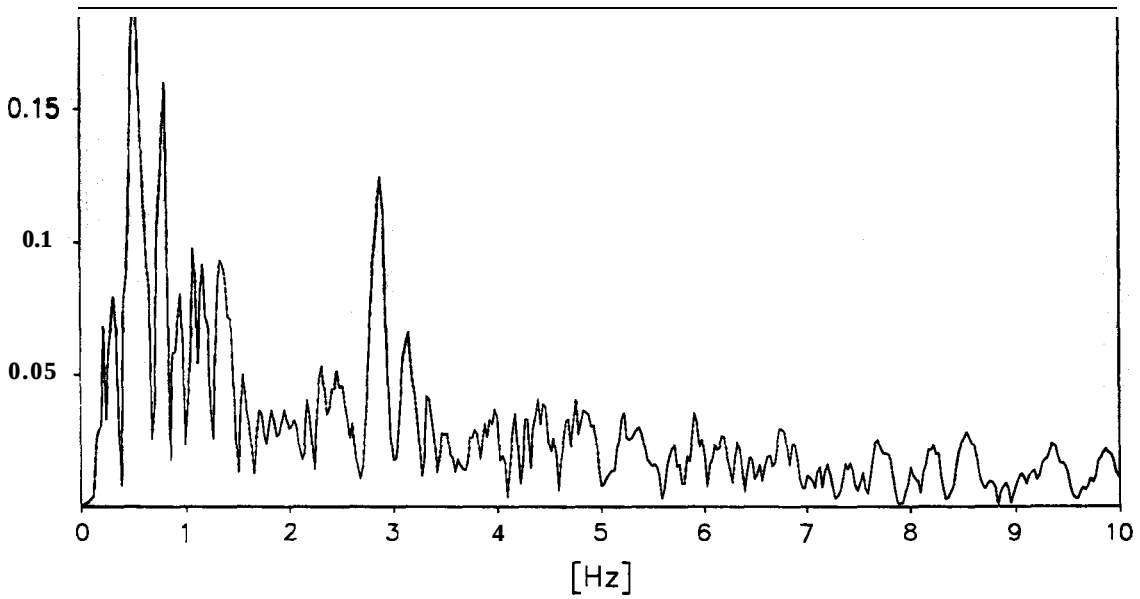

Port Island – Seismograph 32m below ground level

Direction: N-S

TEST MODEL FLIGHT		TIME RECORDS	FIG.NO. 20

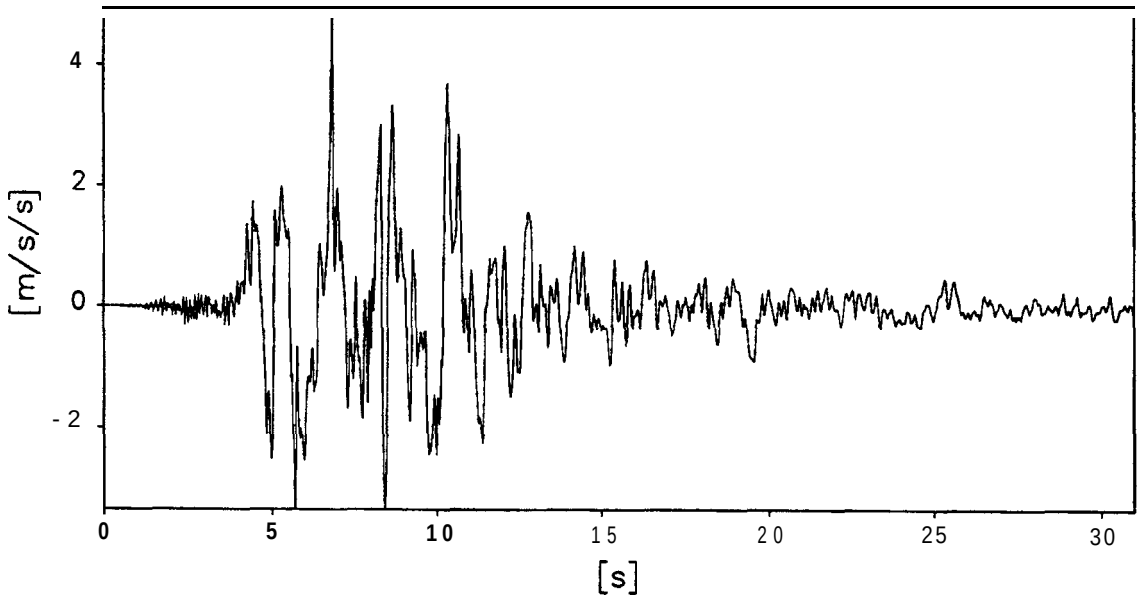

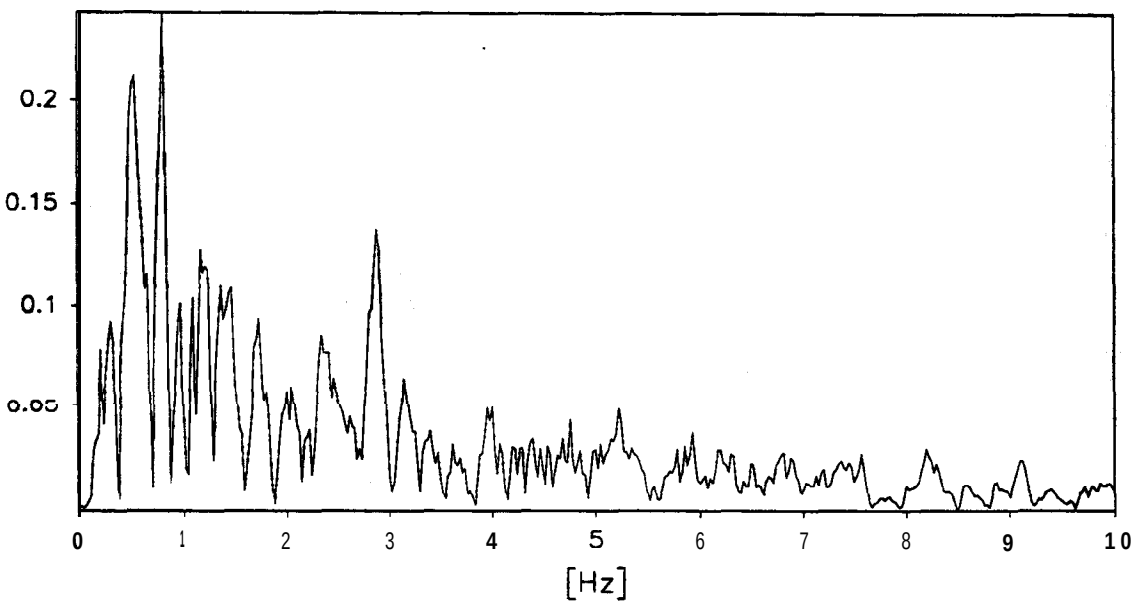

Port Island – Seismograph 16m below ground level

Direction: N-S

TEST MODEL FLIGHT		TIME RECORDS		FIG.NO. 21

data points plotted per complete transducer record

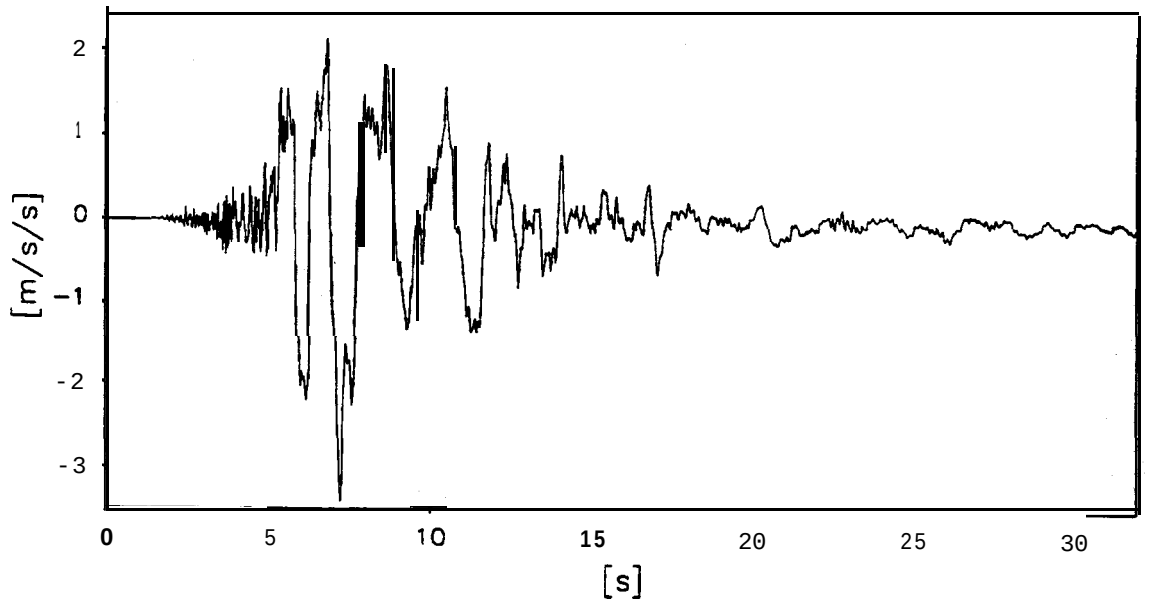

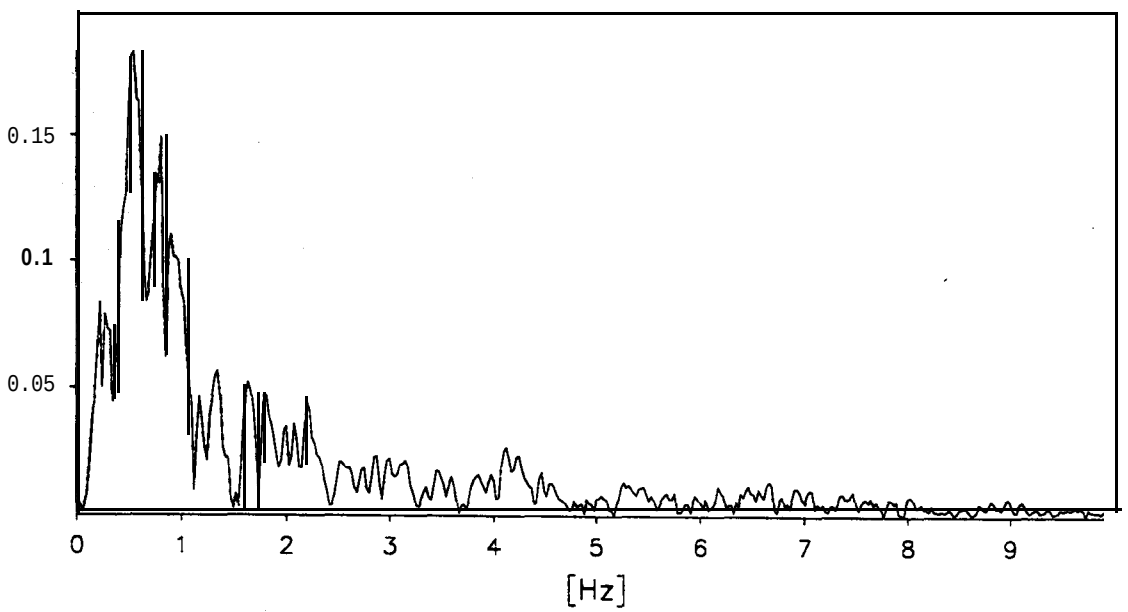

Port Island — Seismograph near ground level

Direction: N-S

TEST MODEL FLIGHT		TIME RECORDS		FIG.NO. 22

7 Frequency Analysis of ground motion in the E-W direction

As in the previous section frequency analyses were carried out by using the Discrete Fast Fourier Transform (DFT) method. In Figs.23 to 26 the frequency analysis of the E-W component and the actual time trace of the strong motion at different depths are presented.

The frequency analysis of the strong motion recorded at the depth of 83 m shows significant components at various frequencies between 0 to 10 Hz as seen in Fig.23. Some of these high frequencies are filtered by the time the strong motion arrives at the depth of 32m. This is seen in Fig.24 which reflects the marked attenuation of the 2.8 Hz component and amplification of the 0.2, 0.5 and 0.75 Hz components. As the strong motion travels upwards to the depth of 16 m the 0.5 and 0.75 Hz components show further amplification as seen in Fig.25. As the strong motion reaches the soil surface there is some attenuation of the 0.5 and 0.75 Hz components as seen in Fig.26. The 2.8 Hz component and all of the high frequency components suffer some attenuation in this region as reflected in Fig.26. Comparing the frequency analyses in Figs. 19 and 22 the dramatic filtering of the high frequency components is visualised.

data points plotted per complete transducer record

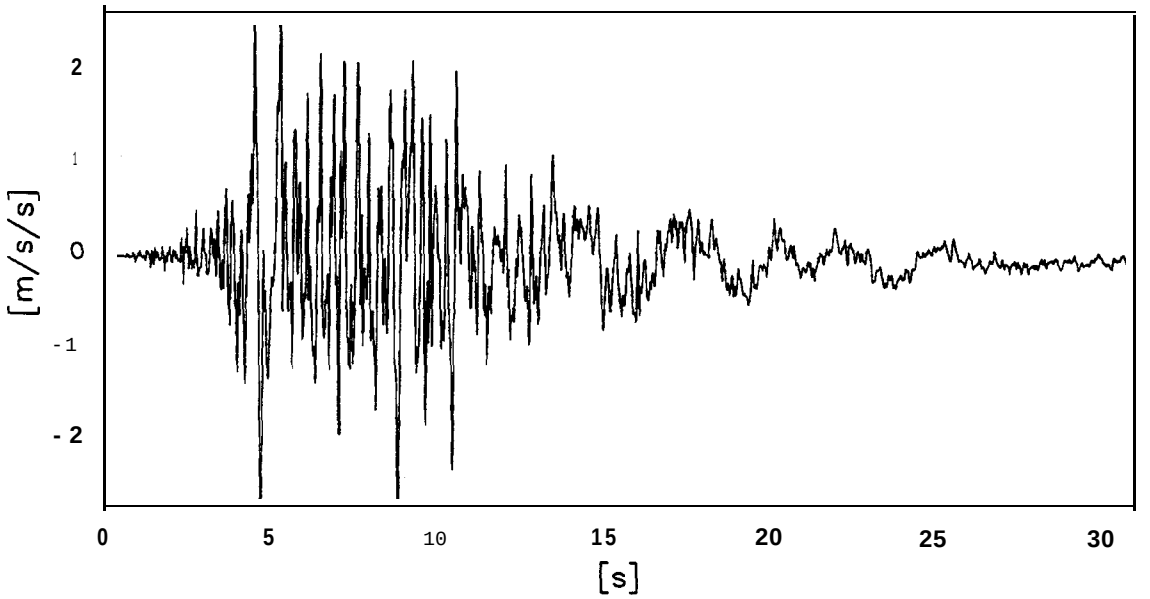

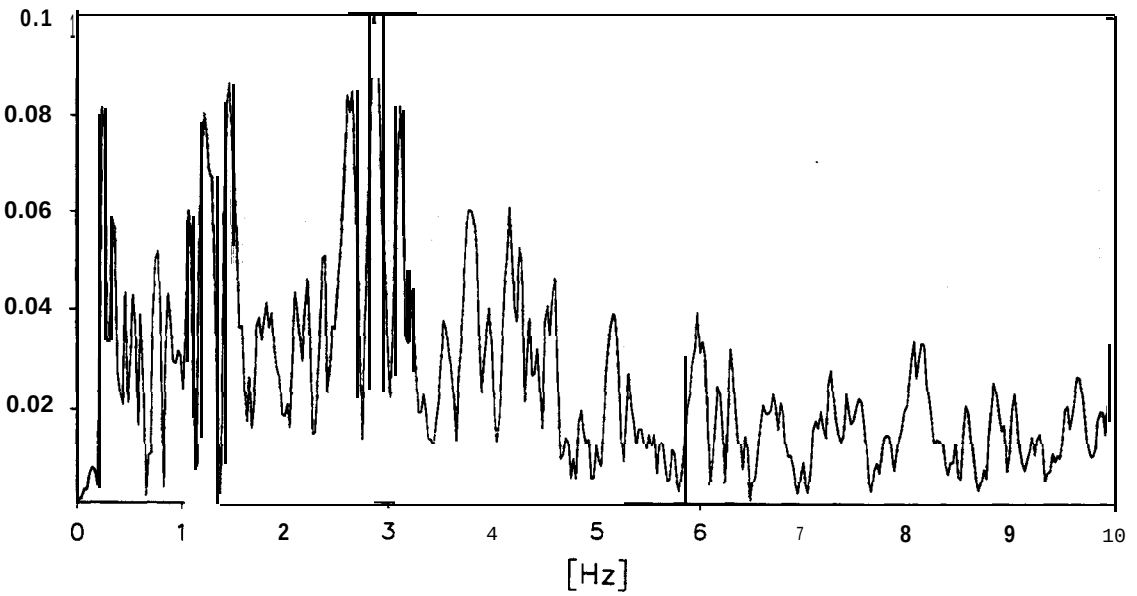

Port Island — Seismograph 83m below ground level

Direction: E-W

TEST MODEL FLIGHT		TIME RECORDS		FIG.NO. 23

data points plotted per complete transducer record

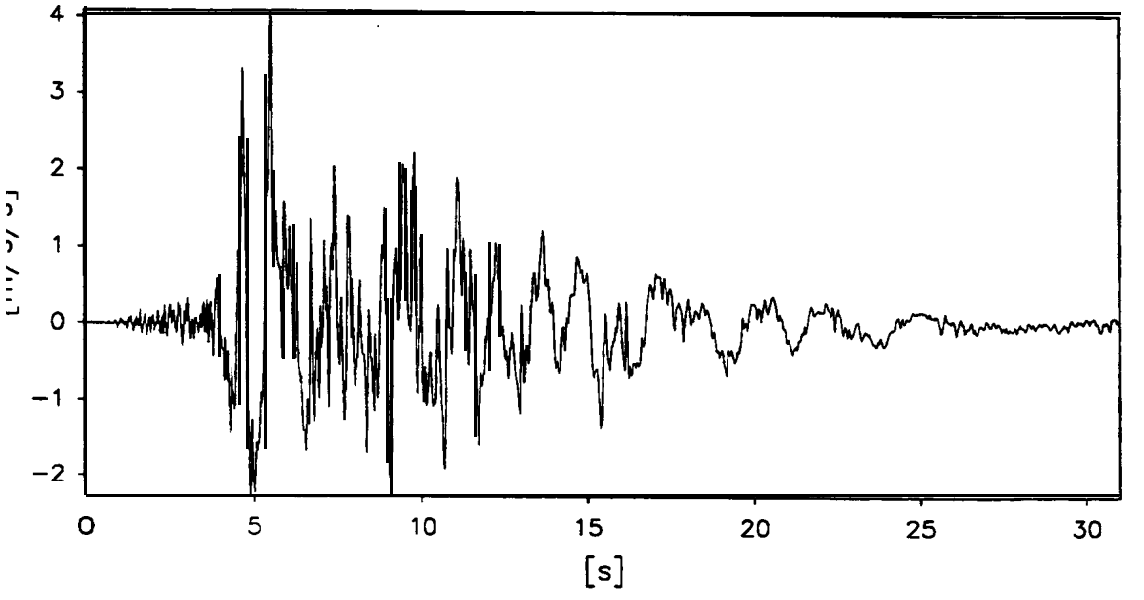

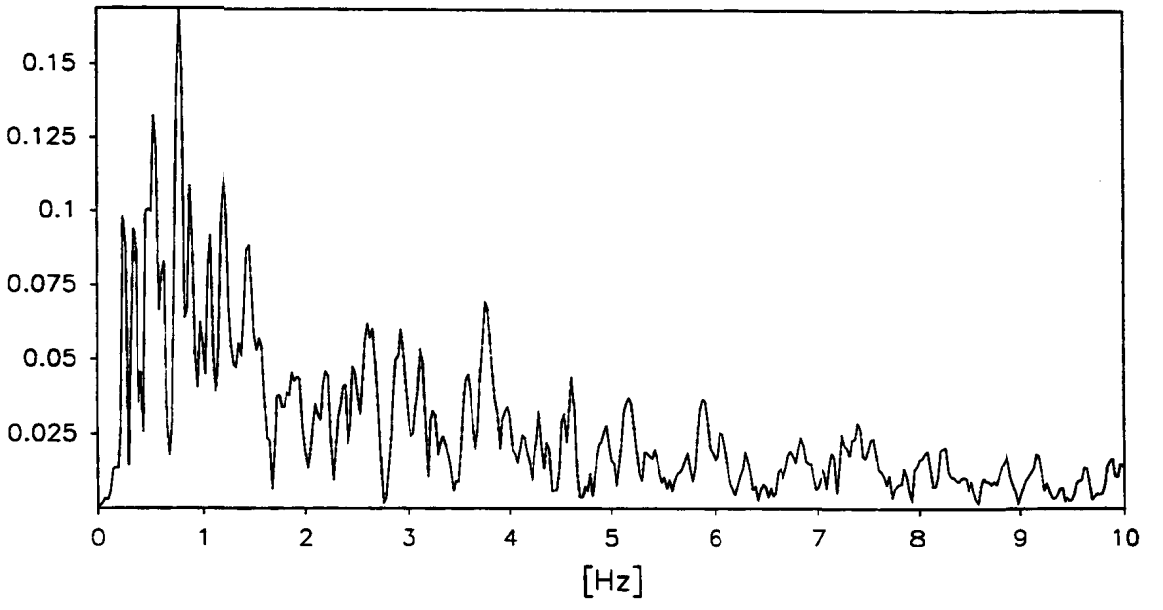

Port sland – Seismograph 32m below ground level

Direction: E–W

TEST MODEL FLIGHT		TIME RECORDS		FIG.NO. 24

data points plotted per complete transducer record

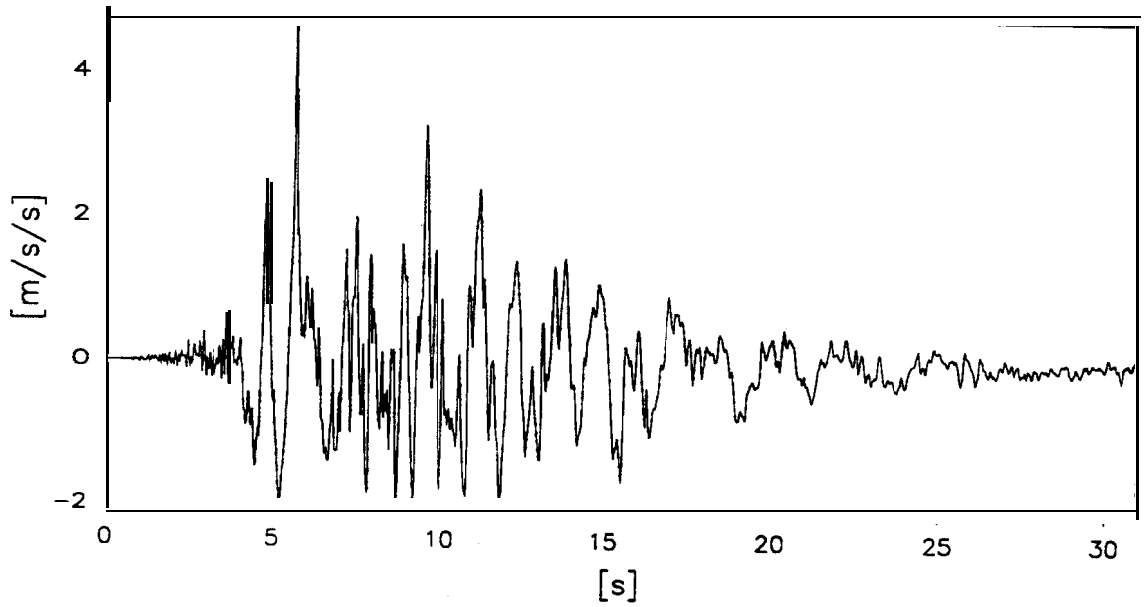

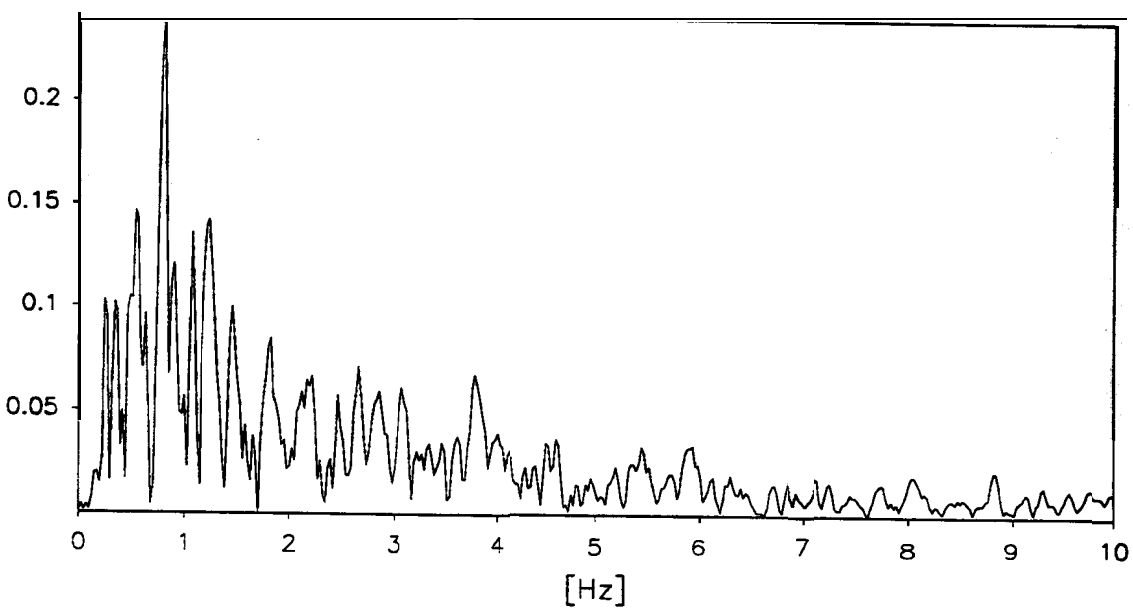

Port sland — Seismograph 16m below ground level

Direction: E—W

TEST MODEL FLIGHT		TIME RECORDS		FIG.NO. 25

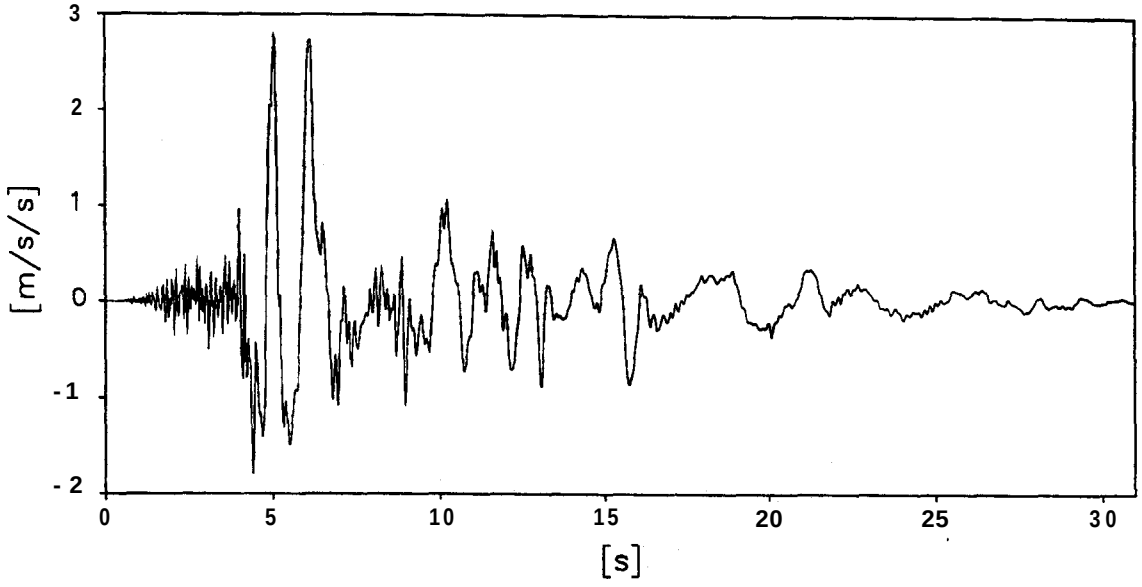

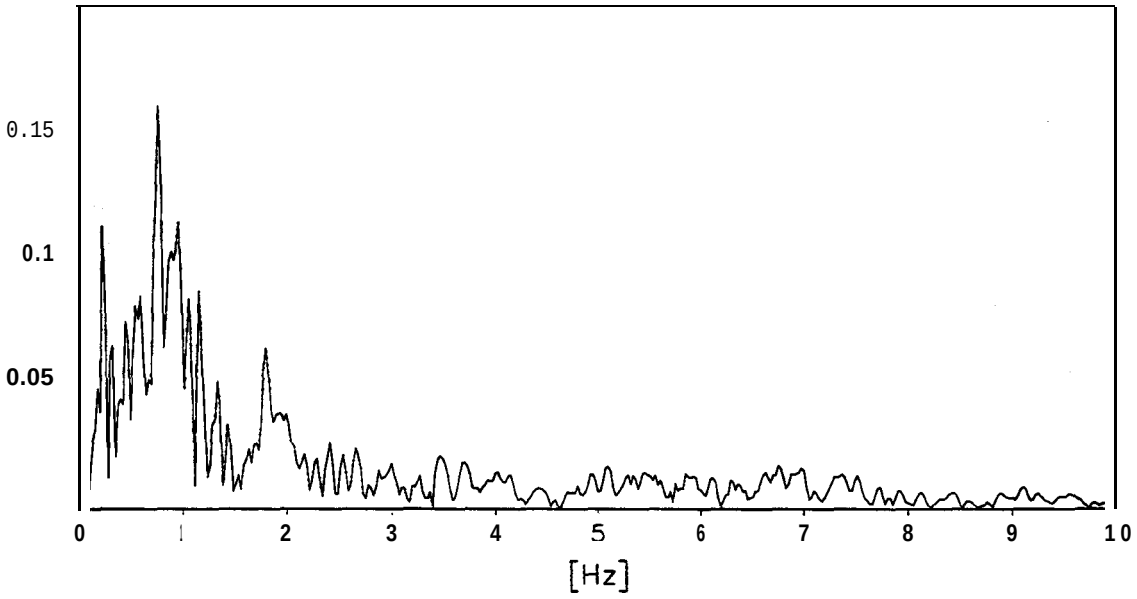

Port Island — Seismograph near ground level

Direction: E-W

TEST MODEL FLIGHT	TIME RECORDS	FIG.NO. 26

8 Frequency Analysis of ground motion in the U-D direction

As in the previous section frequency analyses were carried out by using the Discrete Fast Fourier Transform (DFT) method. In Figs.27 to 30 the frequency analysis of the U-D component and the actual time trace of the strong motion at different depths are presented.

The frequency analysis of the strong motion recorded at the depth of 83 m shows significant components at various frequencies between 0 to 25 Hz as seen in Fig.27. Significantly there are large components between 0 and 2.5 Hz. The frequency components between 2.5 to 5 Hz show amplification by the time the strong motion arrives at the depth of 32m as seen in Fig.28. As the strong motion travels upwards to the depth of 16 m there is an overall amplification at almost all of the frequency components as seen in Fig.29. As the strong motion reaches the soil surface there is further amplification of the 0.5 and 0.75 Hz components as seen in Fig.30.

The pattern of amplification of the vertical accelerations is very different from that of the horizontal accelerations (both N-S and E-W components). This may be expected as they are induced by different kinds of stress waves namely the P-waves and S_h waves as explained in Sec.5.

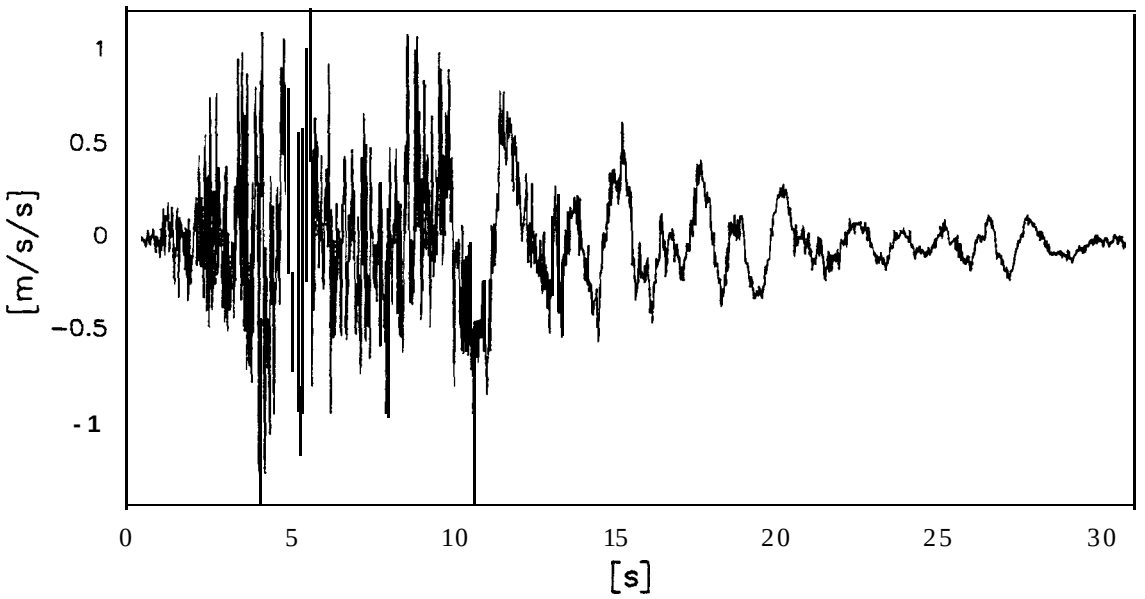

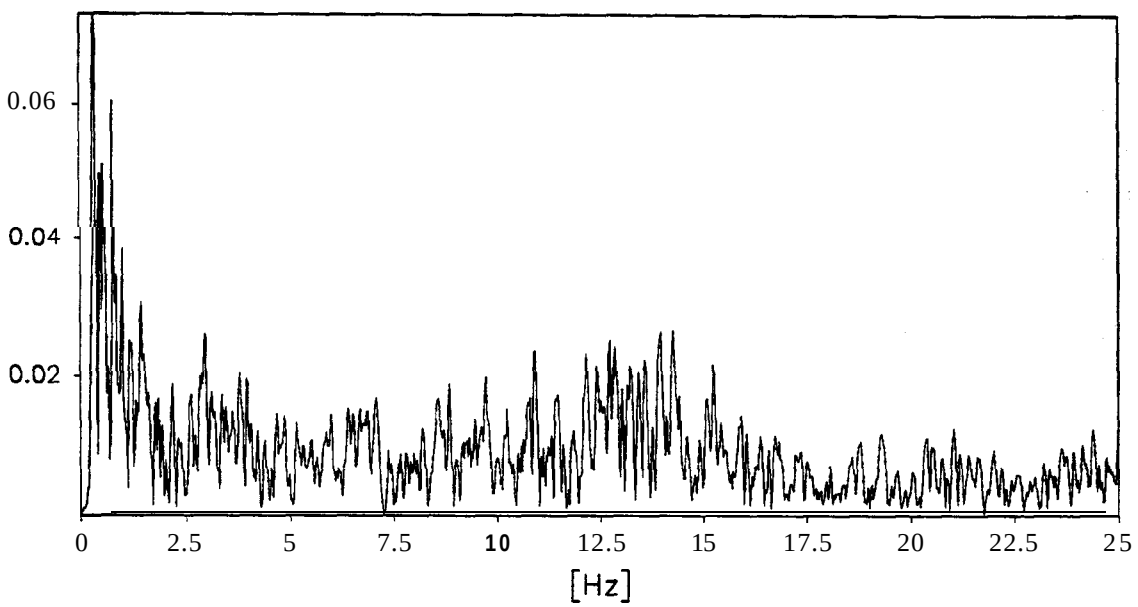

Port Island – Seismogroph 83m below ground level

Direction: **U-D**

TEST MODEL FLIGHT		TIME RECORDS		FIG.NO. 27

dato points plotted per complete transducer record

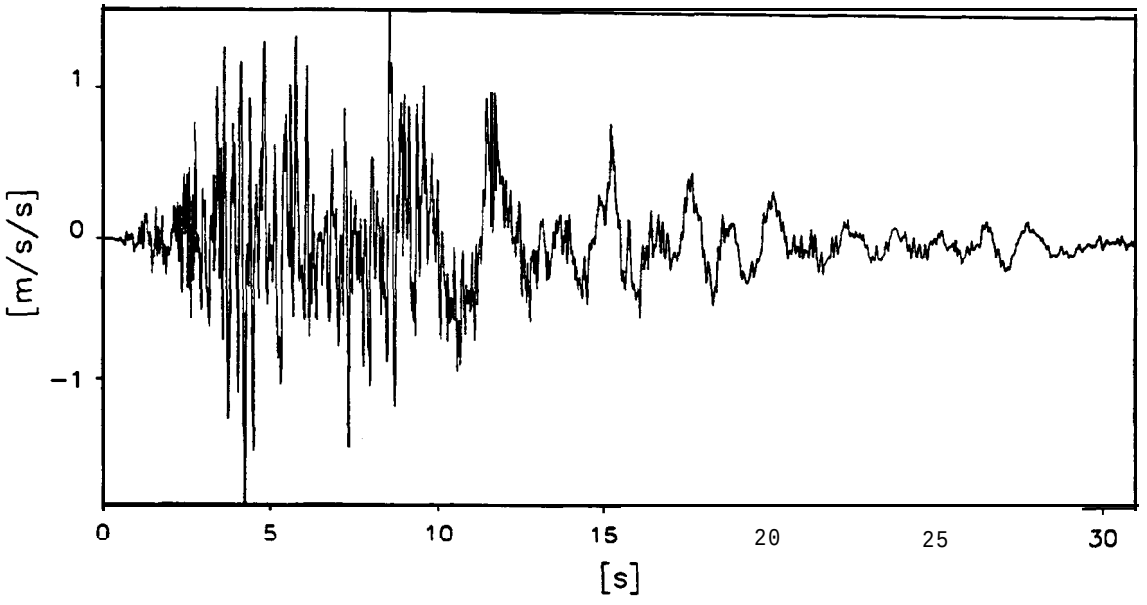

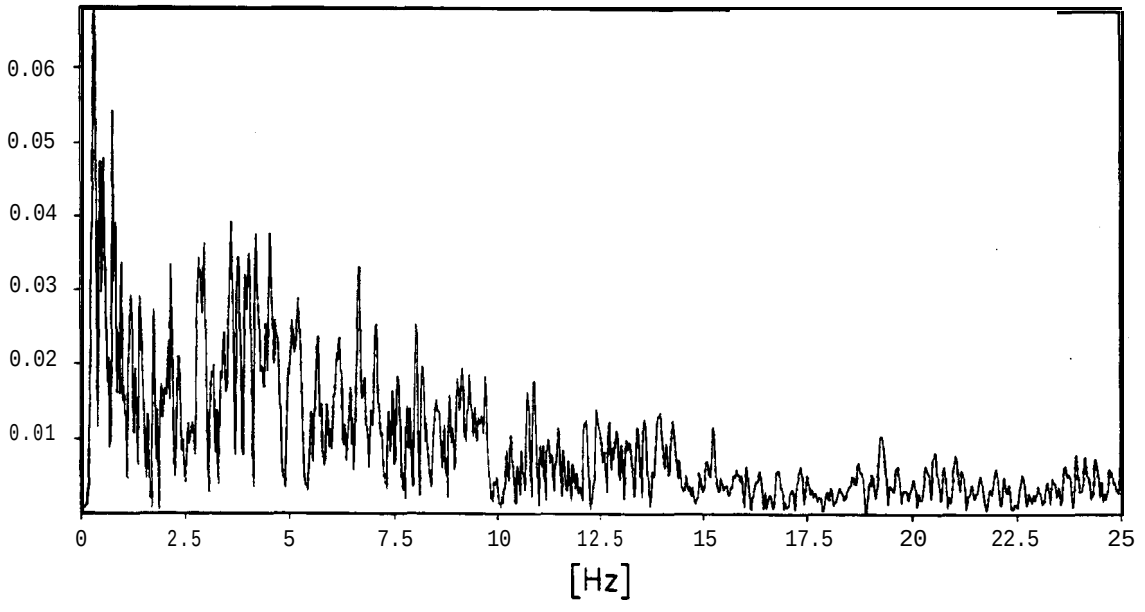

Port Island – Seismograph 32m below ground level

Direction: U-D

TEST MODEL FLIGHT		TIME RECORDS		FIG.NO. 28

data points plotted per complete transducer record

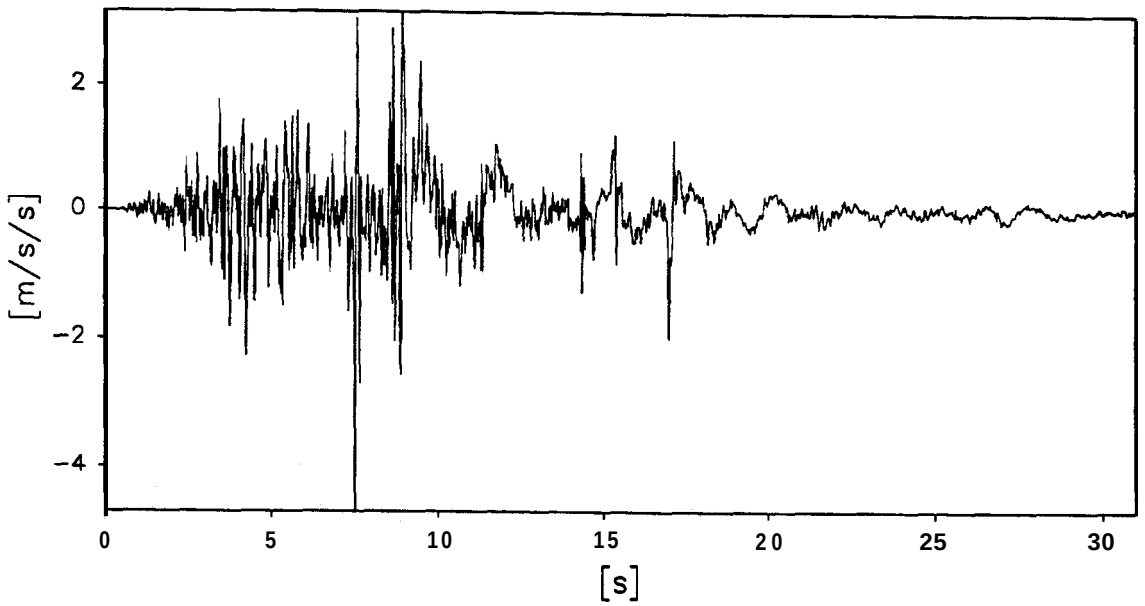

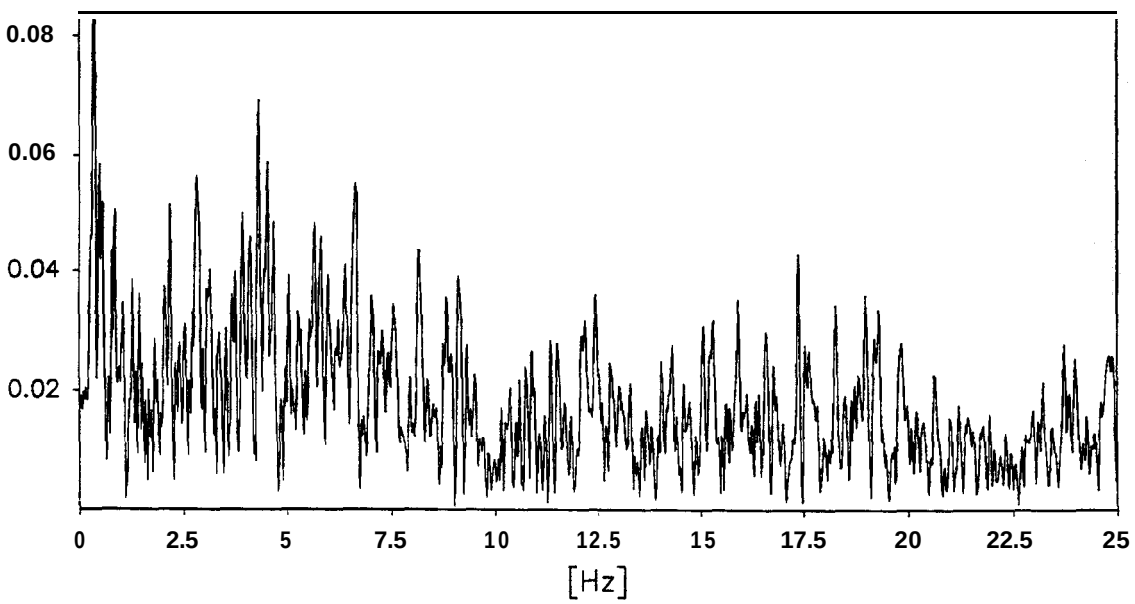

Port Island – Seismograph 16m below ground level

Direction: U-D

TEST MODEL FLIGHT		TIME RECORDS		FIG.NO. 29

data points plotted per complete transducer record

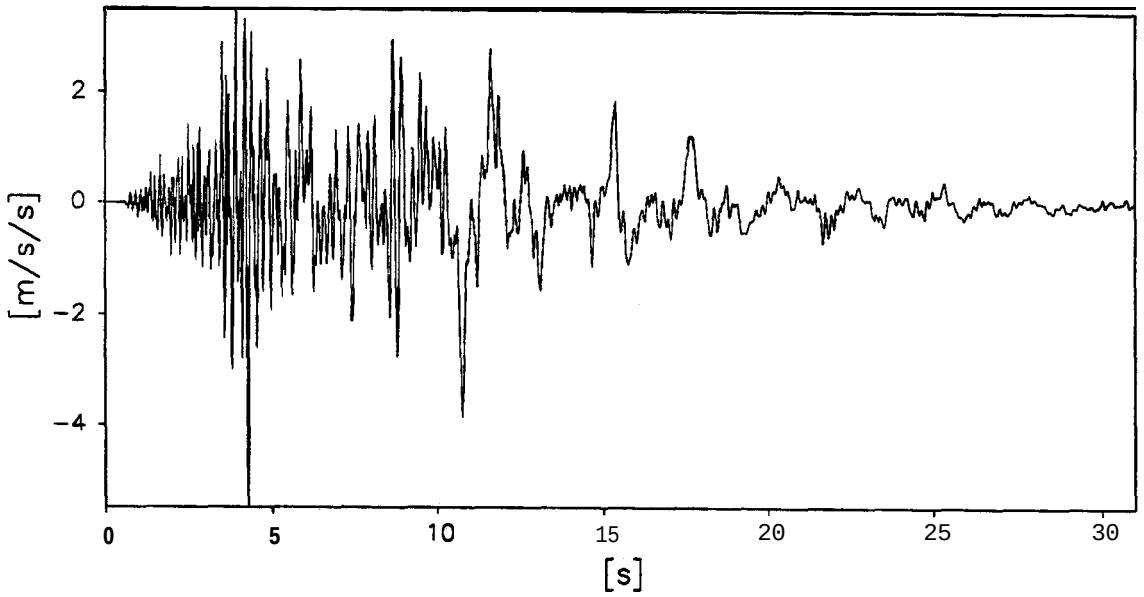

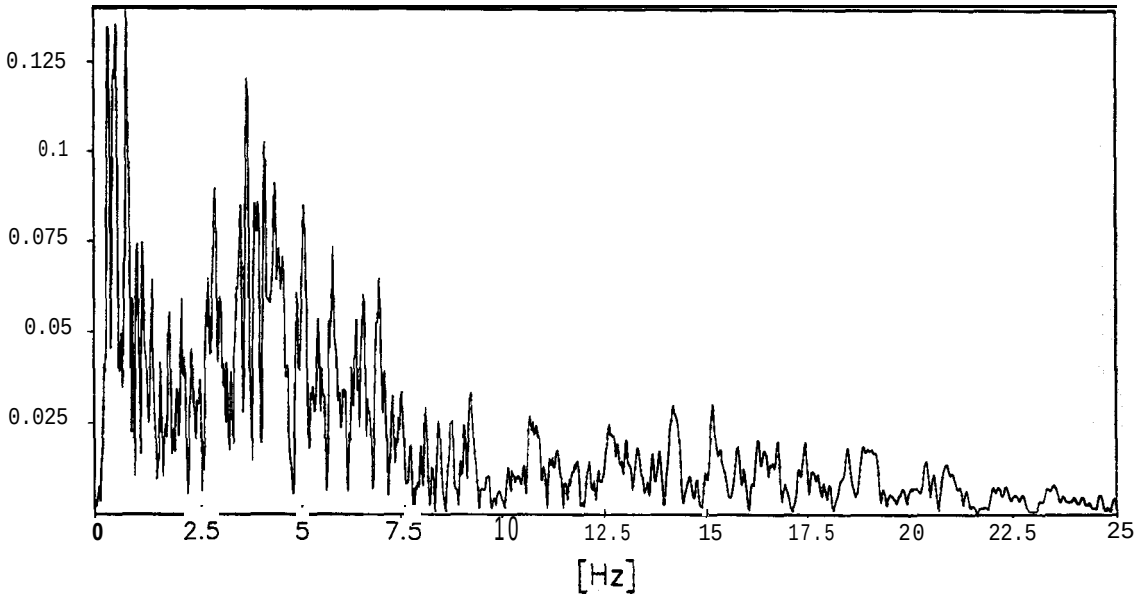

Port Island – Seismograph near ground level

Direction: U-D

TEST MODEL FLIGHT		TIME RECORDS		FIG.NO. 30

8 Implications for modelling of seismic events in a geotechnical centrifuge

Dynamic centrifuge modelling is being extensively used over the past decade in modelling of the seismic events in a geotechnical centrifuge. There is a valid discussion on the type of strong motion that must be used to study the dynamic behaviour of a general soil-structure problem subjected to earthquake loading. Use of servo-hydraulic systems which simulate a 'realistic ground motion' observed in one of the past earthquakes is an approach followed by many universities in the USA like Caltech, RPI, UC Davis and Boulder. One of the difficulties of this approach arises from the fact that use of multi-frequency input may excite various modes of vibration in the mechanical actuators and centrifuge swings. the effects of which are hard to differentiate from the 'real' soil behaviour. An alternative approach used at the Cambridge University is to use a single frequency input to which the system (actuator and swing) response is known. On such system called the Bumpy Road earthquake actuator was used very effectively to study the effects of dynamic soil-structure interaction during earthquake loading, liquefaction induced failures and many such problems. Currently a new system called the Stored Angular Momentum (SAM) actuator is being commissioned which increases the versatility in dynamic centrifuge testing compared to the bumpy road actuator by giving the research worker the choice of frequency of the strong motion and the duration of the earthquake. Also the strength of each earthquake can be varied as desired.

The frequency analyses of the actual horizontal strong motions recorded at the Port Island site as explained in Secs.5 and 6 emphasises the following facts;

I. as the strong motion travels from the bed rock to the soil surface the high frequency components are severely attenuated;

II. specific frequency components of the ground motion show significant amplification relative to the other frequency components (which most probably correspond to the natural frequencies of the soil stratum).

The above facts suggest that it will be more useful to simulate ground motions in the centrifuge which are close to one of the natural frequencies of the soil layer being tested. At Cambridge University it is hoped that the new SAM actuator will be able to impart low intensity earthquakes which sweep a range of frequency. Data from these earthquakes will be used to identify the resonant frequencies of the soil-structure system being investigated. Stronger earthquakes which inflict damage to the soil-structure system will then be fired at one of the eigen frequencies detected in the low intensity sweeping frequency earthquake. This procedure will be repeated to follow the soil-structure system through damaging earthquakes.

9 Conclusions

The strong motion traces recorded at the Port Island site during the Kobe earthquake were analysed. At this site recordings were made in the N-S, E-W and U-D directions at four different depths. The data from these recording provides an excellent opportunity to investigate the modulation of stress waves as they travel from the bed rock to the soil surface. It was observed that there is significant attenuation of the peak ground acceleration in the upper strata of soil at this site. The N-S component and the E-W component during this earthquake are 180° out of phase as the strong motion reaches the soil surface. Lissajous figures of these two components were constructed at all the four depths. These figures suggest that the strong motion polarises in the N-W and S-E direction as the it approaches the soil surface. The arrival times were compared between the U-D components induced by the P waves and the horizontal components induced by the shear waves. As expected the P waves arrive earlier than the shear waves at the soil surface. Frequency analyses were carried out for strong motion recorded in both N-S and E-W directions. These analyses suggest a strong attenuation of high frequency components while selective discrete frequencies are amplified. This suggests that single frequency earthquake actuators may be sufficient, atleast in the initial studies of the dynamic soil-structure interaction problems in a geotechnical centrifuge.

Acknowledgements

The author wishes to express his gratitude to Prof. Andrew Schofield for the helpful discussion on this topic which led to this report. The help rendered by Dr.Kenichi Soga in obtaining the digitised traces of the strong motion from CEORKA is gratefully acknowledged. Also the author wishes to express his thanks for the helpful comments of Dr.Scott Steedman of Sir Alexander Gibb & Partners, Reading.

REFERENCE

Iwasaki , Y., (1995), Strong motion records, CEORKA observation sites, Secretariat, Geo-Research Institute, Osaka, Japan.